Multiple phases of Tertiary extension and synextensional deposition of the Miocene–Pliocene Salt Lake Formation in an evolving supradetachment basin, Malad Range, southeast Idaho, U.S.A.

Sean P. Long[1 *], Paul K. Link[1], Susanne U. Janecke[2], Michael E. Perkins[3], and C. Mark Fanning[4]

[1]*Department of Geosciences, Idaho State University, Pocatello, ID 83209, U.S.A.*

[2]*Department of Geology, Utah State University, Logan, UT 84322, U.S.A.*

[3]*Department of Geology and Geophysics, University of Utah, Salt Lake City, UT 84112, U.S.A.*

[4]*Research School of Earth Sciences, The Australian National University, Canberra ACT, 0200, Australia*

[*]*Correspondence should be addressed to: longsean@isu.edu*

ABSTRACT

The extensional history of the Malad and Bannock ranges in southeast Idaho and northern Utah involves multiple phases of Tertiary normal faulting and synextensional deposition. Detailed geologic mapping, structural and stratigraphic analyses, and geochronologic data from this study elucidate previously defined deformational events in the region, and define two new extensional episodes.

The largest-magnitude extension took place along low-angle normal faults of the ~10–4-Ma Bannock detachment system, with concurrent sedimentation of the Miocene–Pliocene Salt Lake Formation in a regionally continuous supradetachment basin. This basin developed by ~10.2 Ma, and was preceded by two phases of smaller-magnitude, aerially restricted normal faulting and sedimentation. In the Henderson Creek quadrangle of the southern Malad Range, the earliest event involved ~8% north–south extension during deposition of the Paleocene–Eocene Wasatch (?) Formation. This conglomerate unit was deposited in an asymmetric, south-tilted half-graben bounded on the south by the syntectonic Willow Spring normal fault.

The next pre-detachment extensional event produced a north-striking, east-tilted half-graben in which the Middle to Late Miocene Skyline Member of the Salt Lake Formation (~11.9–10.2 Ma) was deposited as an ash-rich alluvial fan. This half-graben is bounded on the east and south by the syntectonic Red Knoll and Spring Trail normal faults. Detrital zircon age data from a tuffaceous sandstone bed in the Skyline Member suggest incorporation of reworked zircons from the ~12.5–15-Ma Owhyee–Humboldt volcanic field in southwest Idaho with 10.3-Ma glass.

The inception of the regional Bannock detachment system is recorded by the breakup and ~16% west-southwest extension of its hanging wall by a set of north- to north–northwest-striking Late Miocene normal faults. These faults were associated with syntectonic deposition of the Cache Valley Member of the Salt Lake Formation (~10.2–<9.2 Ma) in a regional-scale lake system. During deposition, the northeast-dipping Steel Canyon normal fault accommodated uplift of an intrabasinal horst that shed a wedge of Third Creek Member conglomerate eastward into the lake system between ~10.0 and <9.2 Ma. The Third Creek Member interfingers with a Cache Valley Member lake-margin tufa-bearing facies, which changes eastward into a deeper-water facies with micritic limestone.

The most recent extensional event in the Henderson Creek quadrangle involved ~9% east–west extension on the north-striking Pliocene–Quaternary Wasatch fault. A segment boundary of the Wasatch fault, consisting of a 2.5–3.5-km-wide relay ramp that formed between two right-stepping en echelon segments, lies just north of the Idaho–Utah border. In addition, a broad, north- to north–northwest-trending antiformal zone of extensional folds is present in the south half of the study area and is interpreted as a double rollover anticline that formed progressively in Late Miocene and Pliocene–Quaternary time above two oppositely dipping listric normal faults.

KEYWORDS: Bannock detachment system, Basin and Range province, extensional fold, Malad Range, Salt Lake Formation, SHRIMP geochronology, southeast Idaho, tephra correlation, Wasatch fault, Wasatch Formation.

INTRODUCTION

Rocks in southeast Idaho have undergone a complex, multistage Cenozoic extensional history, which has left behind an incomplete structural and stratigraphic record. The Miocene–Pliocene Salt Lake Formation, which is the primary sedimentary record of Late Cenozoic extension in southeast Idaho and northern Utah, crops out in multiple basins throughout the region (Fig. 1). Recent studies have provided radiometric and tephra correlation ages showing that the Salt Lake Formation ranges from Middle Miocene to Pliocene in age (Perkins et al., 1995; Perkins et al., 1998; Goessel et al., 1999; Janecke and Evans, 1999; Oaks et al., 1999; Crane, 2000; Pope et al., 2001; Carney, 2002; Perkins and Nash, 2002; DeVecchio, 2002; Janecke et al., 2003; Long, 2004; Steely et al., 2005). These and other studies of the formation (Mansfield, 1927; Danzl, 1982, 1985; Sacks and Platt, 1985; Link and Stanford, 1999; Rodgers et al., 2002; Biek et al., 2003; Kruger et al., 2003) have helped to characterize the structural and stratigraphic development of Late Cenozoic extensional basins south of the eastern Snake River Plain. However, despite these advances, questions still remain regarding Miocene–Pliocene paleogeography, correlation among isolated Salt Lake Formation exposures, and the Late Cenozoic extensional development of this area of Idaho and Utah.

To better document the deformational timing and style that characterized extension in this region, a geologic mapping study focusing on structural geology and stratigraphy was completed (Long, 2004). The mapping area is located in southeast Idaho, ~110 km south of Pocatello, near the Idaho–Utah border (Fig. 1). This paper and the 1:24,000-scale geologic map of the Henderson Creek 7.5-minute quadrangle (Long et al., 2004) present new data relating to the Late Cenozoic extensional history of the area, particularly the structural, stratigraphic, and age relations of the Salt Lake Formation and other synextensional units (Fig. 2), including the discovery of previously unmapped facies changes associated with Paleocene–Eocene (?) and Miocene syndepositional tectonism. This paper also documents the style, geometry, and kinematics of associated map-scale faults and folds and introduces new interpretations for structures of Paleocene–Eocene (?) to Pliocene–Quaternary age. New Tertiary unit subdivisions, tephra correlation ages, and U-Pb SHRIMP detrital zircon ages are used to document the tectonic setting and timing of deposition, to compare our results to data from other studies (Janecke and Evans, 1999; Carney, 2002; Janecke et al., 2003), and to help categorize extensional events into temporal phases.

REGIONAL GEOLOGY

Pre-rift Geology

Bedrock strata in the Bannock and Malad ranges include volcanic and sedimentary rocks of the Neoproterozoic Pocatello Formation and Brigham Group and westward-thickening Neoproterozoic and Paleozoic sedimentary rocks of the Cordilleran miogeocline (Armstrong and Oriel, 1965). These strata were deformed and translated to the east along west-dipping thrust faults during the Cretaceous to Paleocene Sevier orogeny (Armstrong and Oriel, 1965; Coogan, 1992). The study area is in the hanging wall of the Paris thrust, which is the westernmost major thrust of the Idaho–Wyoming–Utah fold-and-thrust belt (Allmendinger, 1992).

The Wasatch Formation is the name given to red colored, syn- and post-thrust continental strata of the Sevier fold-and-thrust belt (Hayden, 1869; Veatch, 1907; Oriel and Tracey, 1970). In western Wyoming, the unit is syntectonic with movement on the Hogsback thrust fault, the youngest and easternmost of major Sevier thrusts in the region (DeCelles, 1994). However, strata correlated with the Wasatch Formation also exist in the hanging walls of older structures to the west, including the Absaroka, Crawford,

Figure 1, facing page. Simplified geologic map of the Cache Valley, Malad Valley, and Marsh Valley areas. Locations of Henderson Creek quadrangle and other recent Salt Lake Formation mapping studies are shown. Bannock detachment system low-angle normal faults are only exposed on Oxford Ridge, but probably underlie much of the map area. Map modified from Janecke et al. (2003); inset modified from Janecke and Evans (1999).

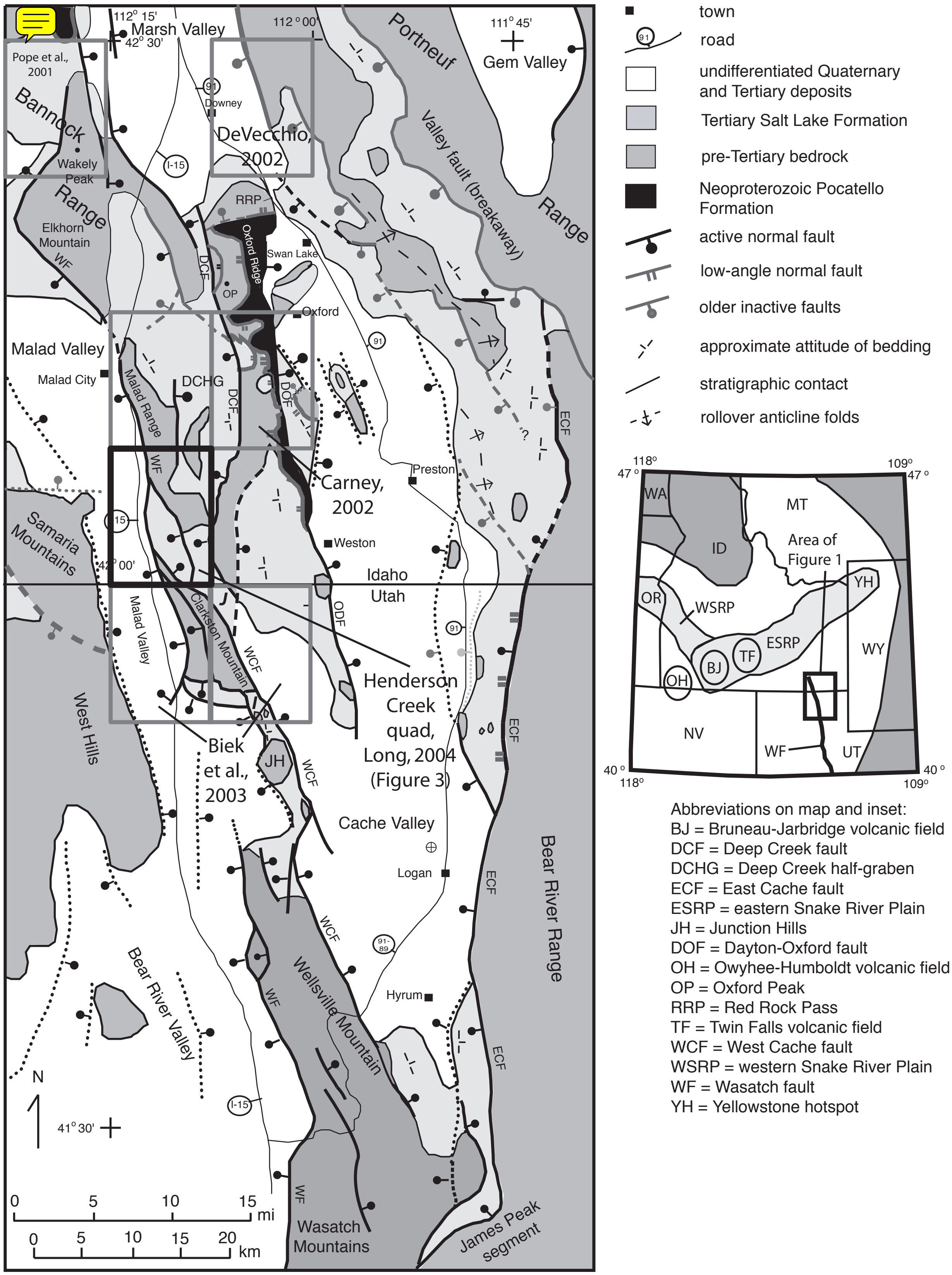
town
road
undifferentiated Quaternary and Tertiary deposits
Tertiary Salt Lake Formation
pre-Tertiary bedrock
Neoproterozoic Pocatello Formation
active normal fault
low-angle normal fault
older inactive faults
approximate attitude of bedding
stratigraphic contact
rollover anticline folds
Pope et al., 2001
DeVecchio, 2002
Carney, 2002
Henderson Creek quad, Long, 2004 (Figure 3)
Biek et al., 2003
Marsh Valley
Gem Valley
Portneuf Range
Valley fault (breakaway)
Bannock Range
Wakely Peak
Elkhorn Mountain
Downey
Swan Lake
Oxford Ridge
Oxford
Malad Valley
Malad City
Malad Range
Preston
Weston
Idaho
Utah
Samaria Mountains
West Hills
Clarkston Mountain
Cache Valley
Logan
Hyrum
Bear River Valley
Wellsville Mountain
Bear River Range
Wasatch Mountains
James Peak segment
Area of Figure 1
0 5 10 15 mi
0 5 10 15 20 km
Abbreviations on map and inset:
BJ = Bruneau-Jarbridge volcanic field
DCF = Deep Creek fault
DCHG = Deep Creek half-graben
ECF = East Cache fault
ESRP = eastern Snake River Plain
JH = Junction Hills
DOF = Dayton-Oxford fault
OH = Owyhee-Humboldt volcanic field
OP = Oxford Peak
RRP = Red Rock Pass
TF = Twin Falls volcanic field
WCF = West Cache fault
WSRP = western Snake River Plain
WF = Wasatch fault
YH = Yellowstone hotspot

and Paris–Putnam thrust systems, where the deposits postdate thrust faulting (Axtell, 1967; Coogan, 1992; Oaks and Runnells, 1992; Goessel et al., 1999; Janecke and Evans, 1999; Carney, 2002; Biek et al., 2003; Long, 2004). The age and stratigraphic relationships between isolated exposures within the hanging wall of the Paris–Putnam thrust and the main body of the unit in western Wyoming have not been synthesized, but the formation appears to record syndepositional Paleocene–Eocene (Jacobson and Nichols, 1982; Lamerson, 1982; Bryant, 1990; DeCelles, 1994) extension and formation of north–south- and east–west-striking horsts and grabens (Oaks and Runnells, 1992).

Late Cenozoic Extension and the Salt Lake Formation

In southeast Idaho, Sevier contraction was followed by Cenozoic extension and the formation of the Basin and Range province. Extension was accommodated through multiple generations of predominantly north-striking normal faults and the development of basins that filled with synextensional deposits of the Salt Lake and Starlight Formations. The name Salt Lake Formation refers to tuffaceous Middle Miocene to Lower Pliocene fluvial and lacustrine strata in southern Idaho and northern Utah (Mansfield, 1920; Oriel and Platt, 1980; Ore, 1982; Miller, 1991; Janecke and Evans, 1999; Link and Stanford, 1999; Goessel et al., 1999; Oaks et al., 1999; Rodgers et al., 2002; Janecke et al., 2003; Biek et al., 2003). The Starlight Formation is the name for correlative, more ash-rich deposits closer to the eastern Snake River Plain (Trimble, 1976; Trimble and Carr, 1976).

The style, geometry, and magnitude of extension that produced the Salt Lake Formation basins vary regionally. Adjacent to the eastern Snake River Plain, two Middle Miocene to Recent extensional phases resulted in ~21% extension across southeastern Idaho by domino-style normal faulting (Rodgers et al., 2002). The first stage, between 15.7 and 9 Ma, produced shallow basins with less than 1,000 m of fill and involved relatively minor extension. During this period, between 16 and 10 Ma, Yellowstone hot spot volcanism was centered to the west at the Owyhee–Humboldt volcanic center, and between 10 and 8.6 Ma, at the Twin Falls volcanic field (Fig. 1) (Pierce and Morgan, 1992). The second and more significant stage of extension near the eastern Snake River Plain took place from ~9 Ma to the present (Rodgers et al., 2002), and resulted in thicker sequences of basin fill. Ages of the fill indicate that extension migrated to the northeast, in front of and adjacent to the Yellowstone hot spot, at roughly the same rate of motion as the hot spot relative to North America (Allmendinger, 1982; Rodgers et al., 2002).

About 100 km to the south, in the Bannock and Malad ranges of Idaho, and in Cache Valley of northern Utah, a different structural style and magnitude of extension is interpreted. Recent studies in these areas (Janecke and Evans, 1999; Carney, 2002; Janecke et al., 2003; Long, 2004; Steely et al., 2005) interpret Late Miocene–Pliocene (~10–4 Ma) extension along low-angle normal faults of the regional Bannock detachment system. Low-angle faults of this system strike north-northwest, dip ~15° west on average, and are only exposed along Oxford Ridge in the southern Bannock Range (Fig. 1) (Link, 1982a, b; Carney et al., 2002; Carney, 2002; Steely et al., 2005). These structures were originally interpreted as contractional (Oriel and Platt, 1979) and later as Mesozoic extensional faults (Link, 1982a, b). They are now interpreted to have been active in the Late Miocene–Pliocene because the faults cut the ~10.2–4-Ma Salt Lake Formation (Janecke and Evans, 1999; Carney, 2002; Janecke et al., 2003). The low-angle faults are interpreted to connect with a proposed breakaway fault zone located ~20 km to the east in Cottonwood Valley (Fig. 1). Overall, the Bannock detachment system accommodated ~15 km of top-to-the-west extension, or 50% extension for the region (Janecke et al., 2003; Carney and Janecke, 2005). The Bannock detachment system is proposed to have originated from extensional collapse of the Cache–Pocatello culmination, a large fault-bend fold that formed above a ramp in the Paris thrust during Sevier thrusting (Rodgers and Janecke, 1992; Carney, 2002; Steely et al., 2005).

Four units of the Salt Lake Formation, which record the structural and stratigraphic evolution of hanging-wall basins of the detachment system, were defined in the Bannock and Malad ranges in previous studies (Fig. 2) (Janecke and Evans, 1999; Carney, 2002; Janecke et al., 2003). In ascending order, these include: (1) the Skyline Member conglomerate; (2) the Cache Valley Member (base at ~10.2 Ma), a tuffaceous and carbonate deposit of a regional-scale lacustrine basin; (3) the Third Creek Member conglomerate; and (4) the New Canyon Member conglomerate. The two younger conglomerate members were deposited in local half-grabens after 10.13 Ma. Clast counts obtained from the conglomerate units have documented progressive unroofing of Paleozoic and Proterozoic strata on Oxford Ridge by the detachment system (Janecke et al., 2003; Steely et al., 2005).

The youngest normal faults in the Idaho–Utah border region are the Pliocene–Quaternary, high-angle basin-and-range faults that control the modern physiography. These faults accommodated ~10% east–west extension, for a total of 60% extension (including the Bannock detachment system component) in the Idaho–Utah border region since the Late Miocene (Carney, 2002; Carney and Janecke, 2005). Major faults from this set include the Dayton–Oxford fault on the west side of Cache Valley, the Deep Creek fault on the west side of the Clifton horst, the East and West Cache faults in central and southern Cache Valley, and the Wasatch fault, which bounds the western side of the Malad Range (Fig. 1).

METHODS

Interpretations of the structural and stratigraphic evolution of the southern Malad Range in this study are based on geologic mapping and photo-geologic interpretation in the Henderson Creek 7.5-minute quadrangle (Fig. 3) (Long et al., 2004). Unit thicknesses and estimates for the percent extension associated with deformational events were obtained from geologic cross sections of the quadrangle (Fig. 4). Clast counts, which involved dividing 100 randomly counted clasts into distinct lithologic groups, were collected from outcrops of conglomerate units of the Salt Lake Formation and from float of loose clasts where no outcrop was available.

Age determinations for units of the Salt Lake Formation were obtained by tephra correlation of volcanic ash samples. Fifteen samples collected in this study were analyzed using the methods of Perkins et al. (1995, 1998). Approximately 20 glass shards per sample were analyzed using an electron microprobe to obtain the percent elemental composition of 13 major elements. Glass shard compositions were then correlated with a database of elemental compositions of regional tuff beds, which had either been directly dated with $^{40}Ar/^{39}Ar$ methods or had an estimated age based on linear interpolation between dated samples.

Eight of the fifteen samples collected in this study were successfully correlated with known ashes. In addition, five other samples from the study area were collected, analyzed, and correlated prior to the beginning of this project (Janecke and Perkins, unpublished data). The results of the 13 successful tephra correlations are presented in Figure 6, shown geographically in Figure 3, and shown stratigraphically in Figure 5. Most ashes are from Yellowstone hot spot eruptions and were probably sourced from the Twin Falls and Bruneau–Jarbridge volcanic fields (Fig. 1).

One tuffaceous sandstone sample from the top of the Skyline Member (37SL03) was analyzed by U-Pb SHRIMP detrital zircon geochronology at the Australian National University, using methods described by Williams (1998) and references therein. Sixty detrital zircon grains were dated, and the results are shown in Figure 7 and Table 1.

STRATIGRAPHY

Pre-Miocene Stratigraphy

Bedrock units in the Henderson Creek quadrangle include sedimentary rocks of the Neoproterozoic–Cambrian Brigham Group and Cambrian–Devonian sedimentary rocks of the Cordilleran miogeocline (Figs. 3 and 4). The most common lithologic units are limestone and dolomite, but shale, feldspathic sandstone, and quartzite units are also present. The full section of Neoproterozoic and Paleozoic rocks exposed within the study area has a post-erosional thickness of ~3,000 m (Long, 2004).

The Paleocene–Eocene (Jacobson and Nichols, 1982; Lamerson, 1982; Bryant, 1990) Wasatch (?) Formation is exposed in the north half of the map area and lies unconformably and in fault contact on Ordovician, Silurian, and Devonian map units (Fig. 3). The formation consists of a pebble-to-cobble conglomerate with a red, mud-rich matrix, which is overlain by mud-rich, unconsolidated beds containing abundant white quartzite boulders up to 6 m in diameter. The maximum exposed thickness of the Wasatch (?) Formation is 189 m, just north of the Willow Spring fault, but the formation abruptly pinches out to the north, and is very thin or absent along the basal Tertiary unconformity south of this fault. We correlate these deposits in the Malad Range with the Wasatch Formation of the Sevier orogenic belt based on the following similarities. The conglomerate

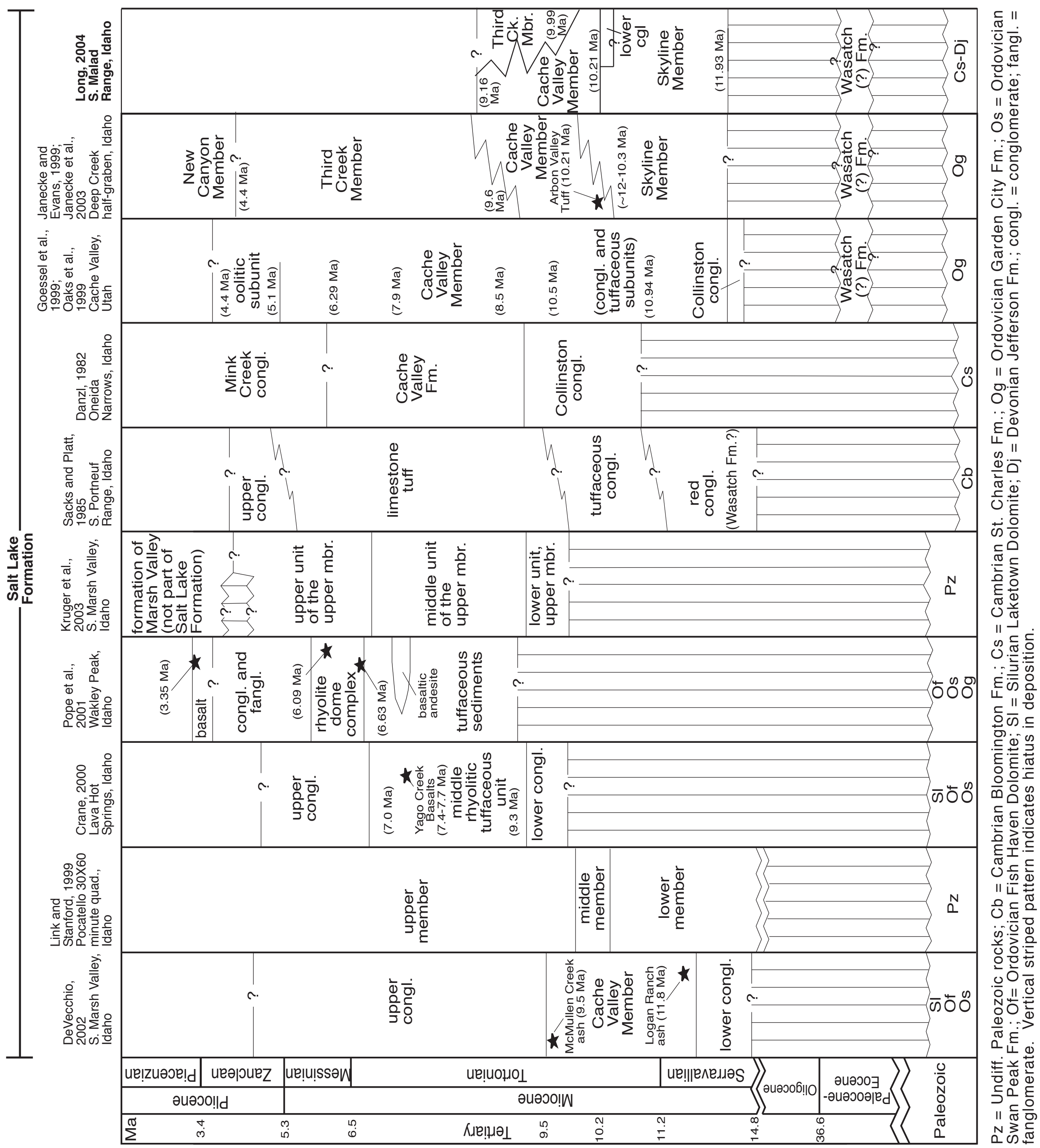

Figure 2. Regional stratigraphic correlation chart for the Salt Lake Formation, showing results from ten studies in southeast Idaho and northern Utah. The stratigraphic column for this study (modified from Long, 2004) is shown on the right. Chart modified from Kruger et al. (2003).

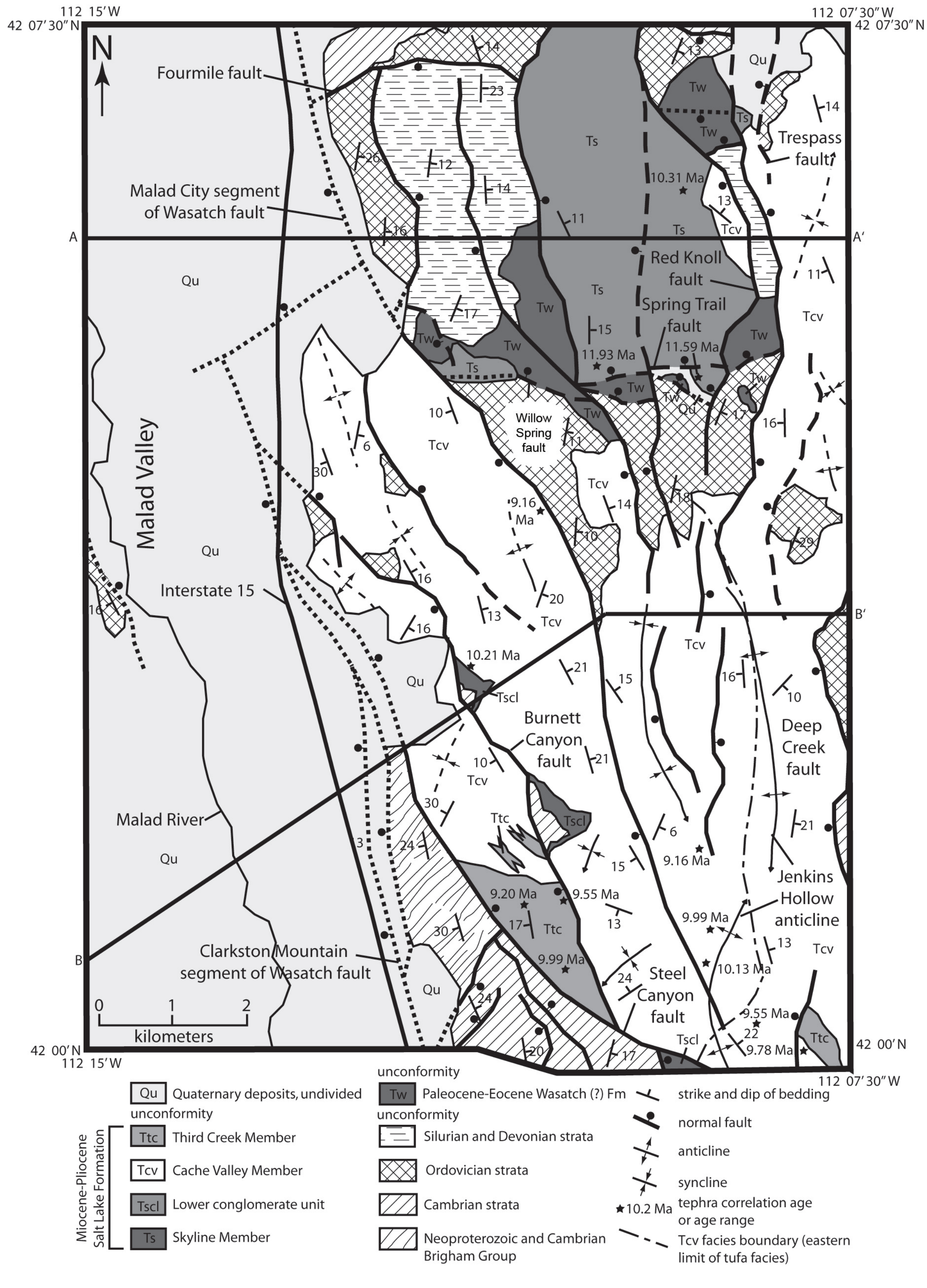

Figure 3. Simplified geologic map of the Henderson Creek quadrangle. Major structures are labeled, along with the locations of the cross-section lines shown in Figure 4. Paleocene–Eocene Wasatch (?) Formation conglomerate and boulder units are combined into one map unit. Tephra sample locations and correlated ages are marked with stars. Tephra sampled for detrital zircons corresponds with the location of the 10.31-Ma sample in the Skyline Member. This map is a simplified version of Long et al. (2004).

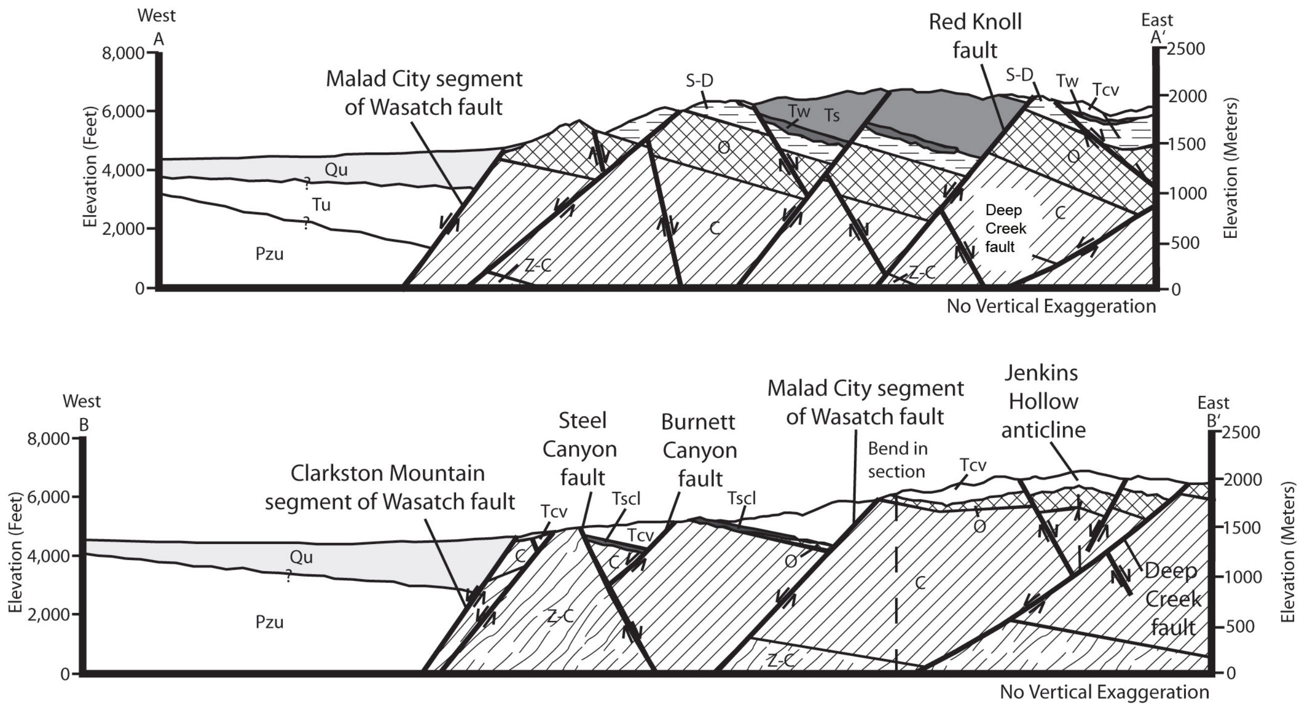

Figure 4. Cross-sections A–A' and B–B' (locations shown in Fig. 3). Undifferentiated Paleozoic (Pzu), Tertiary (Tu), and Quaternary (Qu) units are shown in Malad Valley. The names of major structures are shown. Unit fill patterns are the same as in Figure 3. These are simplified versions of cross-sections from Long et al. (2004).

unit has a similar conglomeratic-to-muddy lithology, similar distinctive red color, the same stratigraphic position below the Salt Lake Formation, and is distinct from the overlying Salt Lake Formation because it lacks ash (Oaks and Runnells, 1992; Goessel et al., 1999; Biek et al., 2003). However, no biostratigraphic or geochronologic data are available to confirm this correlation, and we therefore query the name of the deposits.

Most clasts in the Wasatch (?) Formation conglomerate unit are Silurian and Devonian limestone and dolomite, and are interpreted as locally derived. However, ~20% of clasts consist of tan sandstones and red siltstones of unknown provenance. It is possible that these clasts are derived from the Jurassic Nugget Formation to the east of the map area, or the Pennsylvanian and Permian Oquirrh Formation to the west of the map area. Clasts in the overlying boulder-rich deposits are composed entirely of locally derived Lower Paleozoic clasts.

In the study area, the Wasatch (?) Formation is interpreted as a synextensional deposit related to an east-striking Paleocene–Eocene (?) normal fault set, which contrasts with its syn-thrust origin in western Wyoming and northern Utah (Coogan, 1992; DeCelles, 1994). The conglomerate unit is interpreted to represent deposits of a stream system that flowed parallel to and north of a basin-bounding fault, and the overlying boulder beds are interpreted as locally derived debris-flow and alluvial-fan gravels (Long, 2004). Prior to this study, only Oaks and Runnells (1992) have associated the Wasatch Formation with normal faulting.

Miocene Stratigraphy

The Middle Miocene to Pliocene Salt Lake Formation represents Late Cenozoic synextensional deposition. The cumulative thickness of the Salt Lake Formation varies between 600 and >1690 m in the study area, but exceeds 2 km in the Clifton quadrangle to the northeast (Carney, 2002), and 2.7 km in the Weston Canyon quadrangle to the east (Steely et al., 2005). Within the study area, the Salt Lake Formation is divided into four separate map units (Fig. 5). These include: (1) the Skyline Member conglomerate north of the Willow Spring fault; (2) an unnamed lower conglomerate unit south of the Willow Spring fault; and (3) the lacustrine Cache Valley Member, which interfingers with, (4) the Third Creek Member conglomerate. All units except for the unnamed conglomerate were defined in previous studies in the Bannock

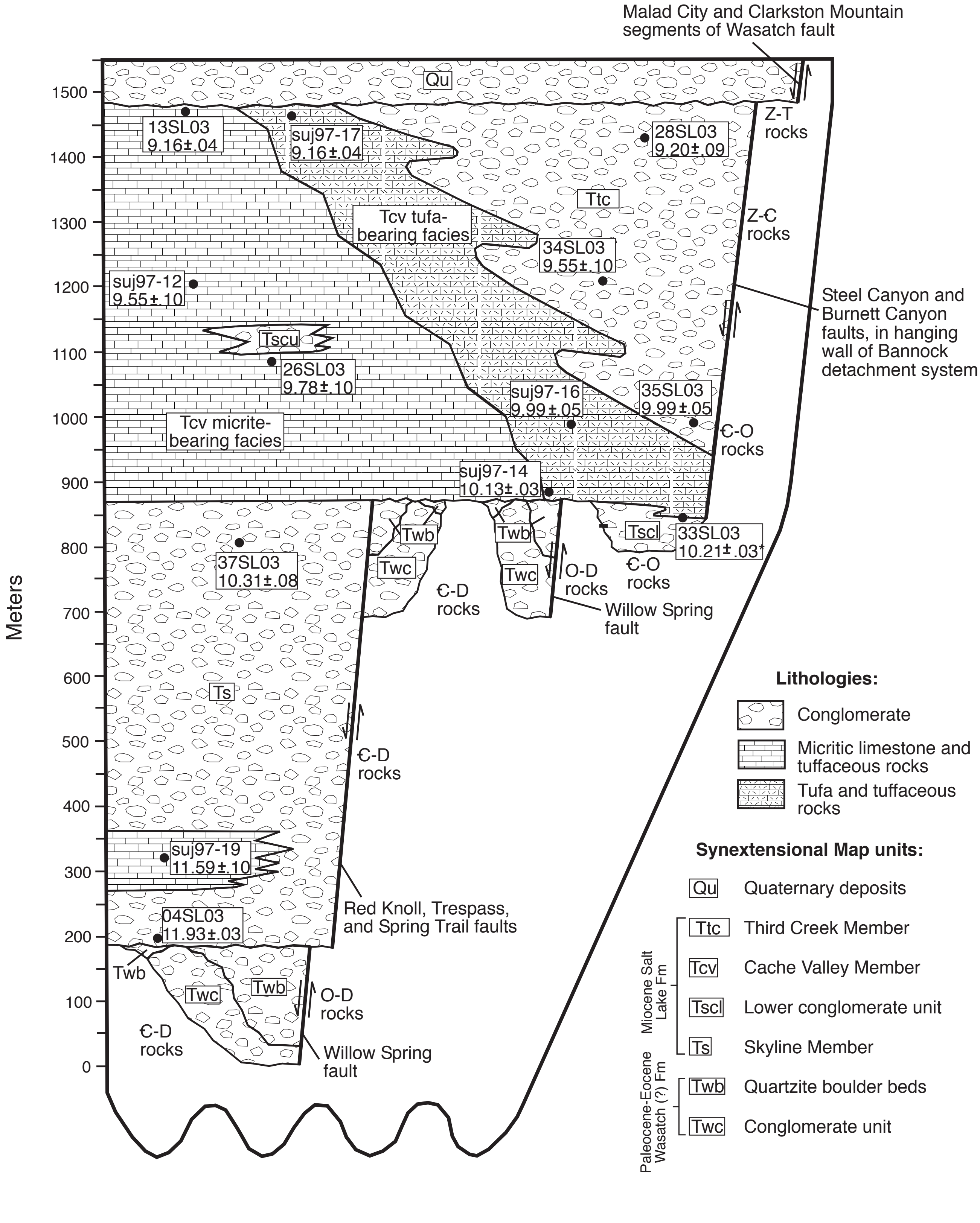

Figure 5. Stratigraphic column of Tertiary synextensional units in the study area. Stratigraphic locations and correlated ages (Ma) of tephra samples, ages of rocks in fault and unconformable contact with Tertiary units, and the names of Tertiary syntectonic normal faults are shown. Figure modified from Long (2004).

Sample Number	UTM Location	Unit	Est. Strat. Position	Correlated Ash Bed	Age (Ma)
13SL03	12T 0402561 4657959	Tcv	upper?	MCM1?	9.16±.04
suj97-17	not available	Tcv	upper?	MCM1?	9.16±.04
28SL03	12T 0402278 4652473	Ttc	middle?	(epb92-75?)	9.20±.09*
34SL03	12T 0402804 4652568	Ttc	lower	Opal Canyon 6?	9.55±.10*
suj97-12	not available	Tcv	middle?	Opal Canyon 6?	9.55±.10*
26SL03	12T 0406068 4650410	Tcv	lower?	Hazen?	9.78±.10*
35SL03	12T 0402909 4652568	Ttc	lower?	(rv88-4?)	9.99±.05*
suj97-16	not available	Tcv	lower?	(rv88-4?)	9.99±.05*
suj97-14	not available	Tcv	lower?	Wooden Shoe Butte tuff?	10.13±.03?
33SL03	12T 0401781 4655400	Tscl/Tcv	contact	Arbon Valley?	10.21±.03
37SL03	12T 0404706 4661834	Ts	upper	(rv88-0?)	10.31±.08*
suj97-19	not available	Ts	lower	Cougar Point Tuff IX?	11.59±.10*
04SL03	12T 0403450 4659894	Ts	lower	Ibex Hollow?	11.93±.03

Figure 6. Chart of successful tephra correlations, showing the sample name, UTM location, estimated stratigraphic location (unit abbreviations are listed on Fig. 3), tuff bed correlation, and correlated age for each sample. Regional ash names from Perkins et al. (1998) are shown where available, and correlative ash bed names are listed. Correlative tuff bed names and GPS locations are unknown for some samples. Samples with an SL03 designation were collected and analyzed for this study; samples with an suj97 designation were collected and analyzed prior to this study (Janecke and Perkins, unpublished data). Sample 33SL03 is the 10.21 ± .03 Ma (Morgan and McIntosh, 2005) tuff of Arbon Valley; this sample was not analyzed, but we are confident of its identification, based on presence of biotite and regional stratigraphy of the Cache Valley Member. Ages with asterisk (*) are interpolated age estimates of possible correlative tephra; all other ages are $^{40}Ar/^{39}Ar$ dates of possible correlative tephra.

and Malad ranges (Janecke and Evans, 1999; Carney, 2002; Janecke et al., 2003).

The total age range of the Salt Lake Formation within the map area is ~11.9–<9.2 Ma (Fig. 6). However, north and northeast of the study area, Salt Lake Formation deposits have been dated between 5.1 and 4.5 Ma, and may possibly be as young as 2 Ma (Janecke and Evans, 1999; Carney, 2002; Janecke et al., 2003).

Skyline Member

The Skyline Member, originally defined in the Malad City East quadrangle to the north (Janecke and Evans, 1999), is the oldest unit of the Salt Lake Formation. This unit is only exposed in the north end of the study area, in a half-graben bounded by the Late Miocene Red Knoll, Trespass, and Spring Trail syntectonic normal faults (Fig. 3). This member consists of poorly exposed, tuffaceous, pebble-to-cobble conglomerate with interbedded tephra and micritic limestone. Tuffaceous matrix material is generally gray or white but is locally altered to green. In rare exposures, medium bedding is most common and beds are more commonly matrix-supported than clast-supported. The thickness of the Skyline Member is estimated from cross section to be up to 685 m. The unit has an age range between 11.93 ± .03 Ma and 10.31 ± .08 Ma, according to tephra correlation data from three ashes (Fig. 6) and the 60 detrital zircon ages (Fig. 7, Table

Figure 7, facing page. SHRIMP age-probability plots for detrital zircons from sample 37SL03 in the upper Skyline Member. ***A***, U-Pb ages of all zircons (n=60). Note scattered ages of the Proterozoic grains. ***B***, U-Pb ages for Tertiary zircons (n = 53). Note presence of two ~11-Ma grains, four Eocene grains, and abundance of ~14.5-Ma grains. ***C***, Weighted average age of 14.54 Ma for Middle Miocene zircons (n = 39).

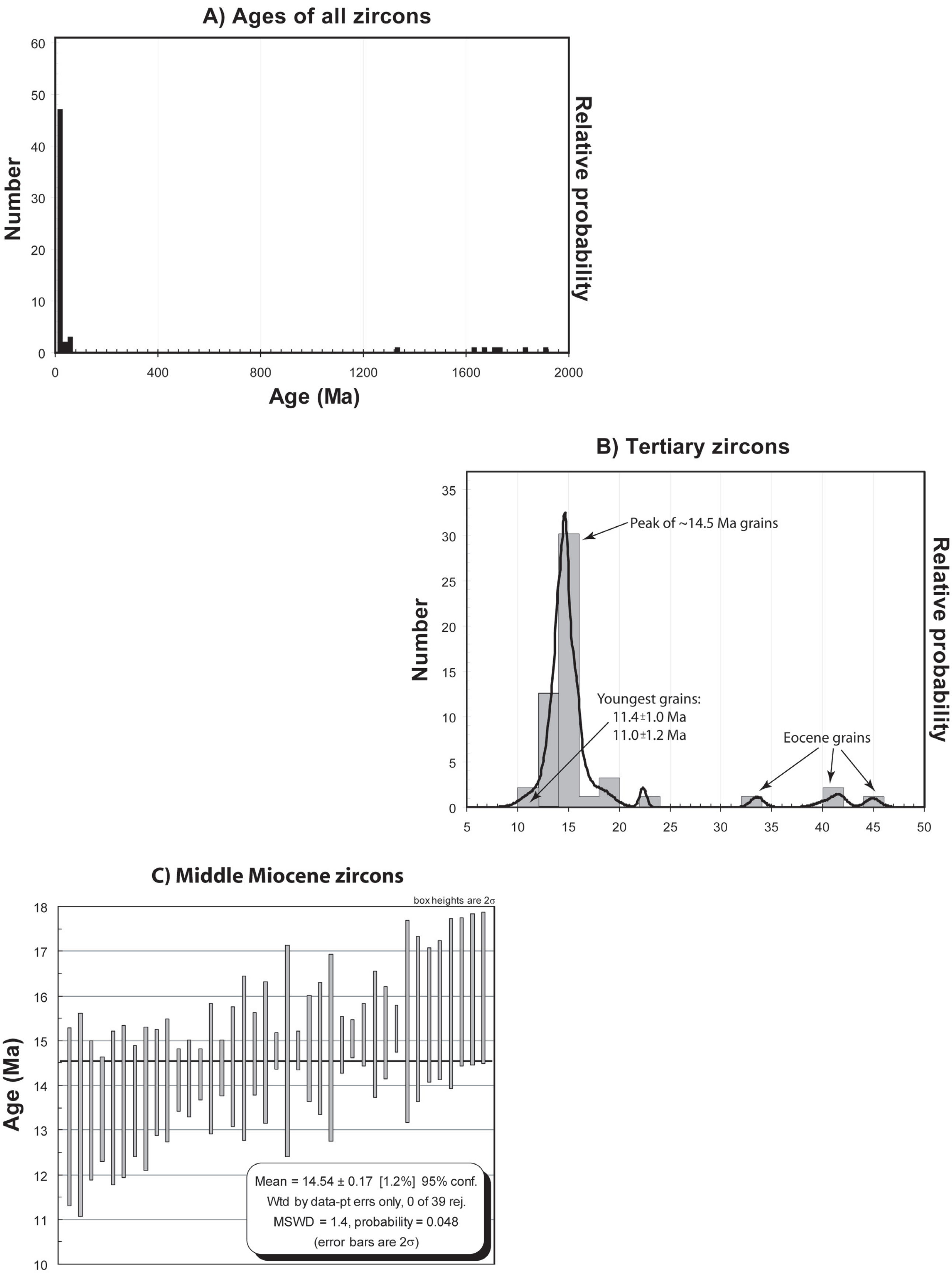
A) Ages of all zircons
Number
Relative probability
Age (Ma)
0
400
800
1200
1600
2000
10
20
30
40
50
60
B) Tertiary zircons
Number
Relative probability
Peak of ~14.5 Ma grains
Youngest grains:
11.4±1.0 Ma
11.0±1.2 Ma
Eocene grains
5
10
15
20
25
30
35
40
45
50
C) Middle Miocene zircons
box heights are 2σ
Age (Ma)
Mean = 14.54 ± 0.17 [1.2%] 95% conf.
Wtd by data-pt errs only, 0 of 39 rej.
MSWD = 1.4, probability = 0.048
(error bars are 2σ)
10
11
12
13
14
15
16
17
18

Table 1. Summary of SHRIMP U-PB zircon analyses for 60 grains from sample 37SL03.

							Total Ratios				Radiogenic Ratios							Age (Ma)				
Grain. spot	U (ppm)	Th (ppm)	Th/U	Pb* (ppm)	$^{204}Pb/^{206}Pb$	f_{206} %	$^{238}U/^{206}Pb$	±	$^{207}Pb/^{206}Pb$	±	$^{206}Pb/^{238}U$	±	$^{207}Pb/^{235}U$	±	$^{207}Pb/^{206}Pb$	±	ρ	$^{206}Pb/^{238}U$	±	$^{207}Pb/^{206}Pb$	±	% Disc
1.1	116	74	0.63	0.2	-	10.40	427.5	23.9	0.1285	0.0134	0.0021	0.0001						13.5	0.8			
2.1	104	64	0.61	0.2	0.011358	10.27	378.2	20.2	0.1275	0.0129	0.0024	0.0001						15.3	0.9			
3.1	3803	2637	0.69	7.6	-	0.46	431.4	6.0	0.0500	0.0013	0.0023	0.0000						14.9	0.2			
4.1	359	208	0.58	0.7	0.001746	4.95	453.2	18.8	0.0854	0.0110	0.0021	0.0001						13.5	0.6			
5.1	252	168	0.67	0.5	-	4.73	439.7	20.3	0.0837	0.0073	0.0022	0.0001						14.0	0.7			
6.1	206	126	0.61	0.4	0.004919	4.53	411.0	17.3	0.0821	0.0128	0.0023	0.0001						15.0	0.7			
7.1	1327	740	0.56	2.5	-	0.17	456.4	8.9	0.0476	0.0023	0.0022	0.0000						14.1	0.3			
8.1	34	41	1.20	10.1	0.000015	0.02	2.896	0.058	0.1167	0.0019	0.3452	0.0069	5.546	0.144	0.1165	0.0019	0.772	1912	33	1904	30	0
9.1	147	131	0.89	0.4	0.000000	14.83	343.7	14.6	0.1636	0.0128	0.0025	0.0001						16.0	0.8			
10.1	146	95	0.65	0.3	0.009582	6.63	388.3	17.9	0.0987	0.0094	0.0024	0.0001						15.5	0.8			
11.1	267	125	0.47	0.5	-	4.39	420.5	15.5	0.0810	0.0085	0.0023	0.0001						14.6	0.6			
12.1	169	118	0.70	0.4	-	5.76	414.5	19.1	0.0918	0.0096	0.0023	0.0001						14.6	0.7			
13.1	3547	2754	0.78	6.9	0.000158	0.56	438.5	6.2	0.0508	0.0014	0.0023	0.0000						14.6	0.2			
14.1	1779	2397	1.35	3.5	0.000722	0.69	434.5	9.0	0.0518	0.0020	0.0023	0.0000						14.7	0.3			
15.1	187	106	0.57	0.4	0.002475	7.69	417.0	17.8	0.1071	0.0088	0.0022	0.0001						14.3	0.7			
16.1	4770	3599	0.75	9.3	-	0.34	440.0	5.8	0.0490	0.0012	0.0023	0.0000						14.6	0.2			
17.1	300	152	0.51	81.0	0.000012	0.02	3.184	0.037	0.1045	0.0006	0.3142	0.0036	4.539	0.059	0.1048	0.0006	0.895	1761	19	1710	11	-3
18.1	359	205	0.57	0.7	-	2.06	420.9	13.5	0.0626	0.0070	0.0023	0.0001						15.0	0.5			
19.1	108	65	0.60	0.2	0.001895	10.39	378.9	25.8	0.1284	0.0131	0.0024	0.0002						15.2	1.1			
20.1	249	141	0.57	0.5	-	5.83	436.1	17.2	0.0924	0.0077	0.0022	0.0001						13.9	0.6			
21.1	99	53	0.53	0.2	0.004770	6.27	386.3	21.7	0.0959	0.0121	0.0024	0.0001						15.6	0.9			
22.1	139	98	0.70	0.4	0.018286	26.92	321.0	13.7	0.2591	0.0162	0.0023	0.0002						14.7	1.0			
23.1	796	353	0.44	1.5	-	2.03	451.8	10.6	0.0623	0.0033	0.0022	0.0001						14.0	0.3			
24.1	5150	2852	0.55	11.0	-	0.36	401.8	5.1	0.0492	0.0010	0.0025	0.0000						16.0	0.2			
25.1	108	47	0.43	0.2	0.013526	9.83	434.6	25.0	0.1239	0.0137	0.0021	0.0001						13.4	0.8			
26.1	391	238	0.61	0.7	0.001657	6.61	451.4	15.2	0.0986	0.0177	0.0021	0.0001						13.3	0.6			
27.1	773	553	0.71	3.5	-	0.65	190.3	3.5	0.0518	0.0022	0.0052	0.0001						33.6	0.6			
28.1	131	66	0.51	0.3	-	6.21	418.4	24.0	0.0954	0.0149	0.0022	0.0001						14.4	0.9			
29.1	165	100	0.61	0.3	0.006711	6.87	411.8	20.6	0.1006	0.0102	0.0023	0.0001						14.6	0.8			
30.1	102	51	0.50	0.3	0.003376	8.30	320.6	18.6	0.1120	0.0192	0.0029	0.0002						18.4	1.2			
31.1	104	52	0.50	0.2	0.003296	5.42	417.5	30.1	0.0891	0.0219	0.0023	0.0002						14.6	1.1			
32.1	1148	855	0.74	2.2	0.000000	1.48	446.4	21.6	0.0580	0.0081	0.0022	0.0001						14.2	0.7			
33.1	422	195	0.46	0.9	-	0.39	388.0	25.5	0.0494	0.0106	0.0026	0.0002						16.5	1.1			
34.1	190	112	0.59	0.3	-	3.33	467.9	25.4	0.0726	0.0119	0.0021	0.0001						13.3	0.8			
35.1	2712	1796	0.66	5.8	-	<0.01	404.7	20.5	0.0457	0.0067	0.0025	0.0001						15.9	0.8			
36.1	424	315	0.74	0.9	0.007158	14.48	418.3	24.1	0.1607	0.0273	0.0020	0.0002						13.2	1.0			
37.1	111	161	1.46	29.8	0.000008	<0.01	3.197	0.069	0.0992	0.0022	0.3154	0.0068	4.612	0.142	0.1061	0.0023	0.700	1767	42	1733	40	-2
38.1	858	784	0.91	2.1	0.005153	1.82	347.5	19.0	0.0608	0.0125	0.0028	0.0002						18.2	1.0			
39.1	1261	1175	0.93	171.1	0.000250	4.38	6.330	0.077	0.1057	0.0008	0.1615	0.0020	2.745	0.061	0.1233	0.0023	0.548	942	12	1666	25	43
40.1	117	89	0.76	0.2	0.004886	4.59	538.5	43.0	0.0825	0.0201	0.0018	0.0001						11.4	1.0			
41.1	1191	731	0.61	1.8	0.001732	1.65	573.8	59.3	0.0593	0.0148	0.0017	0.0002						11.0	1.2			
42.1	873	639	0.73	5.3	0.000000	0.10	142.8	2.3	0.0477	0.0019	0.0070	0.0001						45.0	0.7			
43.1	77	52	0.67	0.1	0.015098	7.50	450.9	33.4	0.1056	0.0268	0.0021	0.0002						13.2	1.1			
44.1	2826	1690	0.60	5.9	0.002415	4.38	408.5	6.3	0.0810	0.0024	0.0023	0.0000						15.1	0.3			
45.1	165	92	0.56	1.9	0.038265	83.53	75.51	2.06	0.7068	0.0234	0.0022	0.0015						14.0	9.4			
46.1	599	409	0.68	1.1	-	1.73	452.1	13.1	0.0600	0.0047	0.0022	0.0001						14.0	0.4			
47.1	250	239	0.96	1.4	0.002126	1.42	156.7	4.0	0.0581	0.0040	0.0063	0.0002						40.4	1.1			
48.1	2516	1662	0.66	7.5	0.000000	0.15	287.5	4.3	0.0477	0.0017	0.0035	0.0001						22.4	0.3			
49.1	5754	4037	0.70	12.0	0.000026	<0.01	413.4	5.3	0.0463	0.0012	0.0024	0.0000						15.6	0.2			
50.1	62	41	0.67	0.2	0.012552	5.98	332.8	23.8	0.0937	0.0241	0.0028	0.0002						18.2	1.4			
51.1	126	44	0.35	24.9	0.000088	0.14	4.336	0.062	0.0820	0.0012	0.2309	0.0033	2.642	0.053	0.0830	0.0012	0.705	1336	17	1269	28	-5
52.1	185	109	0.59	0.4	0.006477	4.91	398.5	18.0	0.0851	0.0093	0.0024	0.0001						15.4	0.7			
53.1	1254	781	0.62	2.4	0.000852	0.87	448.7	9.4	0.0532	0.0029	0.0022	0.0000						14.2	0.3			
54.1	176	60	0.34	50.2	-	<0.01	3.016	0.039	0.1115	0.0010	0.3319	0.0043	5.140	0.082	0.1123	0.0010	0.821	1847	21	1837	16	-1
55.1	153	148	0.97	0.3	0.007923	2.13	464.9	25.9	0.0631	0.0103	0.0021	0.0001						13.6	0.8			
56.1	155	88	0.57	0.3	0.007831	4.90	385.9	18.7	0.0851	0.0101	0.0025	0.0001						15.9	0.8			
57.1	1080	747	0.69	6.0	0.000957	0.31	153.6	2.4	0.0493	0.0018	0.0065	0.0001						41.7	0.7			
58.1	790	452	0.57	1.8	0.007556	12.60	387.2	9.1	0.1459	0.0063	0.0023	0.0001						14.5	0.5			
59.1	995	603	0.61	2.0	0.001006	0.27	429.6	9.6	0.0485	0.0032	0.0023	0.0001						14.9	0.3			
60.1	94	59	0.63	25.0	-	<0.01	3.242	0.049	0.0992	0.0014	0.3087	0.0046	4.252	0.087	0.0999	0.0014	0.738	1734	23	1622	26	-7

Notes :

1. Uncertainties given at the one σ level.
2. Error in FC1 Reference zircon calibration was 0.32% & 0.87% for the two analytical sessions. (not included in above errors but required when comparing $^{206}Pb/^{238}U$ data from different mounts).
3. f_{206} % denotes the percentage of ^{206}Pb that is common Pb.
4. For areas older than ~800 Ma correction for common Pb made using the measured $^{204}Pb/^{206}Pb$ ratio.

1). The Skyline Member lies unconformably on Paleocene–Eocene (?) and Lower Paleozoic units, and its depositional upper contact with the Cache Valley Member is abrupt (Fig. 5).

Clasts of the Skyline Member are almost entirely composed of locally derived lower Paleozoic carbonates, quartzite, and chert (Fig. 8*A*). The Skyline Member is interpreted as an alluvial fan deposit. Based on its poor sorting, clast angularity, locally oversized clasts, and matrix-supported beds, it is interpreted to be the result of braided-stream and debris-flow processes, in accord with earlier interpretations (Janecke and Evans, 1999). The presence of abundant ash from the Yellowstone hot spot, along with dull gray and white matrix color, distinguishes the Skyline member from the underlying Wasatch (?) Formation.

We sampled coarse-grained, green, reworked tuffaceous sandstone (sample 37SL03) located near the top of the Skyline Member for tephra correlation and detrital zircon analysis. Analyses were done using the SHRIMP (Sensitive High Resolution Ion Microprobe) at the Australian National University, using standard techniques for detrital zircon samples (Williams and Claesson, 1987; Compston et al.,1992; Williams, 1998; Link et al., 2005). Each analysis consisted of four scans through the mass range. The data were reduced in a manner similar to that described by Williams (1998, and references therein), using the SQUID Excel Macro of Ludwig (2003).

The 60-grain detrital zircon plot (Figs. 7*A* and *B*) shows 7 Proterozoic grains (12%), 4 Eocene grains (7%), and 49 Miocene grains (82%). Thirty-nine of the Miocene grains are Middle Miocene and have an average age of 14.54 ± 0.17 Ma (Figs. 7*B* and *C*, Table 1). Two ~11-Ma grains constrain the oldest possible age of the sample. Surprisingly, the best tephra correlation for 18 glass shards in the same sample is with a 10.31 ± .08-Ma tuff (Fig. 6). Since the shards are younger than the bulk of the zircons, this suggests that the sample represents mixing of detrital zircons from a stream system draining Proterozoic, Eocene, and Miocene (14.5–11 Ma) sources, with glass shards (but no zircons) derived from a 10.3-Ma fallout tuff eruption.

The closest and most likely source area for the ~14.5-Ma detrital zircons is the 12.5–15-Ma Owyhee–Humboldt volcanic field of southwestern Idaho (Fig. 1). The Proterozoic zircons may have been sourced from Paleozoic strata of southern Idaho that contain these recycled zircons, or from uplifted Proterozoic metamorphic rock, possibly from the Albion–Raft River core complex (Link et al., 2005). We suggest that this sample represents mixing of zircons from a fluvial system that drained eastward from northern Nevada and southwest and south-central Idaho (Link et al., 1999; Beranek, 2005), with fallout tuff from a 10.3-Ma eruption.

Lower conglomerate unit

The lower conglomerate unit of the Salt Lake Formation is a poorly exposed, tuffaceous, pebble-to-cobble conglomerate that crops out only in the southern half of the map area, south of the Willow Spring fault (Fig. 3). While no tephra beds from this unit were sampled, its lies stratigraphically below an ash that was lithologically correlated to the distinctive 10.21 ± .03-Ma (Morgan and McIntosh, 2005) tuff of Arbon Valley (Figs. 5 and 6). Bedding is medium-to-thick, and matrix-supported beds

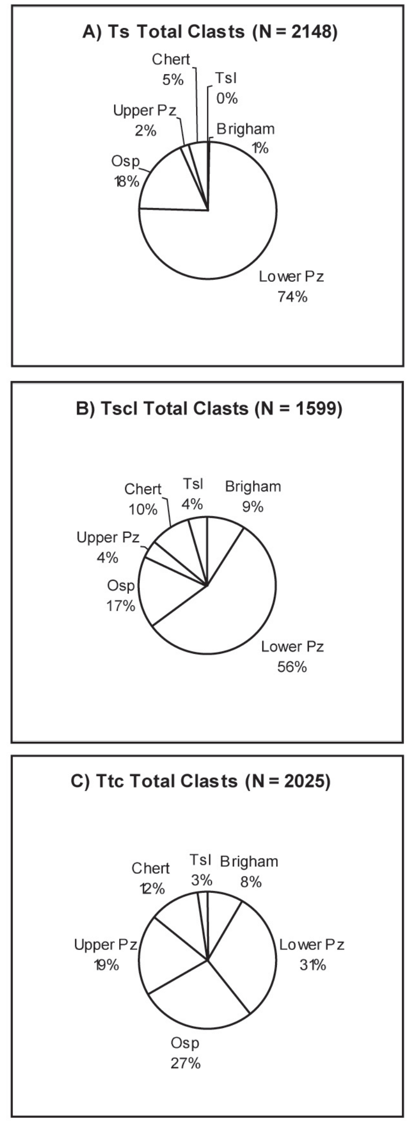

Figure 8. Pie diagrams showing clast count data for: ***A***, Skyline Member (Ts), ***B***, lower conglomerate unit (Tscl), and ***C***, Third Creek Member (Ttc). Lithologic groups are: chert, recycled Salt Lake Formation (Tsl), Brigham Group, Lower Paleozoic, Upper Paleozoic, and Ordovician Swan Peak quartzite (Osp). Figure modified from Long (2004).

are more common than clast-supported beds. Like the Skyline Member, this unit also displays local green zeolitic alteration of normally white and gray tuffaceous matrix material. Its exposed thickness is variable, with a maximum of 66 m. This conglomerate unit lies unconformably on Cambrian and Ordovician rock units, and its upper contact with the Cache Valley Member is gradational (Fig. 5). The unit pinches out to the north, indicating the presence of a drainage divide between this shallow basin and the Skyline Member half-graben.

Clasts in the lower conglomerate unit consist mostly of Lower Paleozoic carbonates, quartzite, and chert, with lesser Neoproterozoic quartzite and Upper Paleozoic calcareous sandstone and limestone (Fig. 8*B*). The Upper Paleozoic clasts were probably sourced from exposures to the west in the Samaria Mountains area (Platt, 1977). The presence of 4% recycled tuffaceous Salt Lake Formation clasts within the conglomerate (Fig. 8*B*) may indicate a partial source from the Skyline Member to the north, which would require the base of the lower conglomerate unit to be younger than ~12 Ma. The lower conglomerate unit represents a thin, basal layer that filled low-relief paleovalleys in the south half of the Henderson Creek Quadrangle prior to 10.2 Ma. Based on its moderate sorting, locally well-rounded clasts, and the presence of Upper Paleozoic clasts probably derived from the west, this unit may have been deposited by an east-flowing stream system.

Cache Valley Member

The Cache Valley Member, the most widely exposed unit of the Salt Lake Formation, consists of a thick section of interbedded lacustrine limestones, tufas, tuffaceous siltstone and sandstone, and primary tephra beds. Tuffaceous beds and ash fall deposits represent ~60% of the unit. Studies of the Cache Valley Member north and northeast of the map area (Janecke and Evans, 1999; Carney, 2002) document the presence of extensive green zeolitic alteration of tuffaceous lithologies, suggesting periodic saline-alkaline lake conditions. In the Henderson Creek quadrangle, green alteration is locally present, but not nearly as prevalent.

The thickness of the Cache Valley Member is estimated from cross section to be >610 m. Tephra correlation data from seven different samples show that the member was deposited between 10.21 ± .03 Ma and <9.16 ± .04 Ma (Fig. 6). In the southern part of the map area, biotite-bearing tuff beds that correlate with the 10.21-Ma Arbon Valley Tuff Member of the Starlight Formation lie at or near its base. The Cache Valley Member lies in unconformable contact on Lower Paleozoic and Paleocene–Eocene (?) units, in depositional contact with the two basal conglomerate units of the Salt Lake Formation, and interfingers with the conglomerate of the Third Creek Member (Fig. 5).

Due to the presence of root tubules, caliche nodules, algal laminations, and fossils, we interpret the Cache Valley Member as a shallow lake deposit. This lake was regional in scale and is interpreted to have formed above the subsided, coherent hanging-wall block of the Bannock detachment system, shortly after its inception (Janecke et al., 2003). The tufa-rich facies of the member, which dominates the western half of exposures, contains abundant macro- and microfossils (ostracodes, gastropods and pelecypods), and abundant rhizoliths. These deposits probably represent lake-margin bioherms (Ford and Pedley, 1996) and may also be associated with hydrothermal circulation along active faults. The tufa facies grades laterally to the east into a facies dominated by medium-bedded micritic limestone and tuffaceous rocks. This facies may represent deeper-water deposits that are more distal to the lake margin. The tuffaceous siltstone-rich section of the Cache Valley Member farther north in the Malad City East quadrangle exhibits extensive green zeolitic alteration, and likely represents deeper-water, periodically saline-alkaline portions of the lake (Janecke et al., 2003).

Third Creek Member

The conglomeratic Third Creek Member of the Salt Lake Formation is exposed in the southern end of the map area, in close proximity to a major Late Miocene structure, the Steel Canyon fault (Fig. 3). This unit interfingers with the Cache Valley Member along strike (Fig. 5). Tephra correlation data show that the Third Creek Member is between 9.99 ± .05 and <9.20 ± .09 Ma, which is the same age as the upper 80% of the Cache Valley Member (Figs. 5 and 6). The Third Creek Member consists of pebble-to-cobble conglomerate with a tuffaceous matrix and a minimum exposed thickness of 381 m. Clasts are subangular to rounded and moderately sorted; bedding is medium to thick and locally massive; and beds are more commonly matrix-supported than clast-supported. Sedimentary structures in the conglomerate include small-scale, tangential cross bedding, scour surfaces, graded bedding, and upward-fining sequences. Clasts in the Third Creek Member are mostly Brigham Group quartzites and Lower Paleozoic carbonates, quartzites, and chert (Fig. 8*C*), which are currently exposed in the footwall of the Steel Canyon fault (Fig. 3). However, nearly 20% of the clasts are Upper Paleozoic sandstone and limestone, probably derived from exposures in the Samaria Mountains area to the west (Platt, 1977). The presence of 3% recycled tuffaceous and carbonate Salt Lake Formation clasts suggests local incorporation of reworked and uplifted beds of the Cache Valley Member.

The Third Creek Member is interpreted as a clastic wedge sourced from the footwall highlands of the active Steel Canyon fault, based on facies and clast count evidence in the structural geology section listed below. The presence of well-rounded and well-sorted clasts near the base of the Third Creek Member may indicate a beach or stream environment, and the interbedded nature of the contact with the Cache Valley Member may indicate that fluvial and beach systems were only active during lake lowstands.

STRUCTURAL GEOLOGY

Four separate sets of normal faults, each representing different episodes of Tertiary extensional deformation, are present in the study area. The oldest fault set includes east-striking normal or strike-slip faults interpreted as Paleocene–Eocene (?) in age based on field relations with the Wasatch (?) Formation. The youngest fault set consists of Pliocene–Quaternary basin-and-range structures that cut across all older faults and bound modern topographic features. Intermediate in age between these two fault sets are a set of north- to north–northwest-striking Middle to Late Miocene normal faults, interpreted to be syntectonic with the deposition of the Salt Lake Formation. Most structures of this set are interpreted to be associated with Late Miocene hanging-wall deformation above the Bannock detachment system. However, a subset of syntectonic normal faults associated with the Skyline Member is thought to represent an isolated Middle-to-Late Miocene extensional event that preceded slip on the Bannock detachment system and produced an east-tilted half-graben in the northern part of the quadrangle.

Paleocene–Eocene (?) Normal Faults

A set of east-striking normal faults is exposed in the north half of the study area (Fig. 3). These faults are cut by Miocene and younger structures, and were responsible for an estimated 8% north–south extension. Certain faults of this set show evidence for pre- or syn-Wasatch (?) Formation displacement. For this reason, we interpret this fault set to be Paleocene–Eocene (?) or older in age, and to represent the earliest episode of Tertiary extension. It is also possible that some structures of this set may have originated as tear faults associated with Sevier orogeny thrusting, but no kinematic indicators were found to support this interpretation.

One major structure from this set, the Willow Spring fault, shows evidence for slip during deposition of the Wasatch (?) Formation. First, the fault has an estimated dip-slip displacement of over 850 m for Paleozoic units, but the offset of the Wasatch (?) Formation is much less. Second, the conglomerate and boulder units of the Wasatch (?) Formation in the hanging wall both increase in thickness in proximity to the fault. Third, the boulder unit is present on both sides of the Willow Spring fault, and the conglomerate unit is only present in the hanging wall. Finally, the boulder unit overlies Ordovician rocks in the footwall of the Willow Spring fault, and Silurian- and Devonian-age rocks in the hanging wall. This means that significant uplift and erosion of the footwall must have occurred between the time of fault slip initiation and the time of deposition of the boulder unit.

In addition to syn-Wasatch (?) Formation slip, parts of the Willow Spring fault may have been reactivated in the Middle to Late Miocene. The east-striking Spring Trail fault (Fig. 3), which formed the southern edge of the half-graben in which the Skyline Member of the Salt Lake Formation was deposited, may connect with the Willow Spring fault at depth, and may represent a Miocene reactivation of the Paleocene–Eocene (?) structure (see discussion below).

Middle to Late Miocene Normal Faults

The Red Knoll, Trespass, and Spring Trail faults (Fig. 3) are interpreted as Miocene structures that formed the north-striking ~12–10-Ma Skyline Member half-graben, prior to development of the Bannock detachment system (Janecke et al., 2003). The Red Knoll fault is the main fault of this set; this structure has a variable north-northeast to northwest strike, and probably has a planar down-dip geometry, based on the lack of folding of the Salt Lake Formation in its hanging wall. Along the majority of its length, the Red Knoll fault places the Skyline and Cache Valley Members on Paleocene–Eocene (?) and older units (Fig. 3). Dip-slip on the Red Knoll fault is estimated at a maximum of 915 m.

The following field relations show that the Skyline Member records syntectonic sedimentation during motion on the Red Knoll fault. First, unit thicknesses change markedly across the fault; in the hanging wall, an extensive exposure of the Skyline Member is estimated at over 680 m thick, while a much thinner section of the Skyline Member (<100 m) is present within its footwall. Second, less than 1 km east of the Red Knoll fault, in the footwall of the Trespass fault, the Skyline Member is absent, and the Cache Valley Member is in depositional contact with Paleozoic and Eocene units. Janecke and Evans (1999) also showed that the Skyline Member is completely absent east of the Red Knoll fault just to the north of the map area. Based on these relationships, the Red Knoll and Trespass faults are interpreted to have been active during deposition of the Skyline Member between 11.9 and 10.2 Ma. However, both faults also cut the base of the Cache Valley Member, so they either remained active after 10.2 Ma, or were both reactivated at a later time.

Dip-slip on the Red Knoll fault decreases significantly south of the east-striking Spring Trail fault. This structure truncates against the Red Knoll fault on its east end, and forms the square-shaped southern boundary to the Skyline half-graben. The Spring Trail fault merges with the east-striking Paleocene–Eocene (?) Willow Spring fault on its western end (Fig. 3). The Spring Trail fault may represent a reactivation of part of the Willow Spring fault, and the two may be connected at depth. Also, given its orthogonal strike to the Red Knoll fault, it is possible that the Willow Spring fault is a transfer structure or an oblique-slip normal fault with a significant strike-slip component, but no kinematic evidence was found to support this interpretation.

Late Miocene Normal Faults

Structures of the Late Miocene normal fault set generally strike north and north-northwest, and dip both west and east. Dip angles for these structures vary between 40° and 67°, and west-dipping faults generally have a slightly shallower dip. Fault spacing varies between 200 and 2,000 m, and dip-slip displacement for nearly all of the structures of this fault set is on the order of 100–1000 m. Cross-section restorations indicate that these faults, along with the Middle to Late Miocene faults associated with the Skyline half-graben, were responsible for 16% east–west extension of the map area. Certain faults of this set, such as the Steel Canyon fault described below, are interpreted to be syntectonic with the Late Miocene Cache Valley and Third Creek members of the Salt Lake Formation.

The Steel Canyon fault is a northwest-striking, northeast-dipping Late Miocene normal fault that is exposed in the southern half of the map area (Fig. 3). This structure is antithetic to the top-to-the-west low-angle normal faults of the Bannock detachment system. Synthetic faults dominate the hanging wall of the detachment system, but antithetic faults are also documented farther east (Carney and Janecke, 2005). The dip of the Steel Canyon fault is estimated at 67°, and its geometry is interpreted as listric, based on field relations that suggest rollover of the Salt Lake Formation in parts of its hanging wall. Estimates of dip-slip displacement along the fault vary from 450 to 1,900 m, and show that throw may increase to the northwest. The Steel Canyon fault places the Cache Valley and Third Creek members of the Salt Lake Formation on Neoproterozoic and Cambrian rocks throughout its length.

Facies relationships within the Salt Lake Formation suggest that the Steel Canyon fault was active during deposition of the Cache Valley and Third Creek members. First, the western part of exposures of the Cache Valley Member, within 5 km of the Steel Canyon fault, are dominated by ledge-forming tufa deposits, which are interpreted as a shallow-water, lake-margin facies (Fig. 3). Second, most of the Third Creek Member was only deposited within 1 km of the Steel Canyon fault (Fig. 3), where it interfingers with the Cache Valley Member. The Third Creek Member is interpreted to represent coarse alluvial deposits shed off of the footwall highlands of the active structure. Third, clast counts within the Third Creek Member show that clasts compatible with footwall derivation increase in number and coarsen with proximity to the structure (Fig. 9). Moving upsection in the unit, toward the Steel Canyon fault, a 108% increase in the number (Fig. 9*A*) and a 34% increase in the average size (Fig. 9*B*) of footwall-derived Brigham Group and Lower Paleozoic clasts is observed, and most clasts show a poorer degree of sorting and an increase in angularity. These three lines of evidence suggest that this fault was active for the majority of Late Miocene deposition. Since the Third Creek Member is only present along a fraction of the fault trace, the Steel Canyon fault is interpreted as an intrabasinal fault rather than a basin-bounding structure.

Pliocene–Quaternary Basin-and-Range Normal Faults

The youngest set of faults in the map area formed during the basin-and-range phase of high-angle normal faulting. The main structures from this set are the Clarkston Mountain and Malad City segments of the Pliocene–Quaternary Wasatch fault, which define a faulted, right-stepping relay ramp (Fig. 3). These structures were responsible for ~9% east–west extension of the map area since the Pliocene, indicating that the Henderson Creek quadrangle has been extended 25% in this direction since the Middle Miocene.

The Wasatch fault is a regional-scale, active, north-striking, west-dipping normal fault system that runs from central Utah, along the Wasatch Front, to southeast Idaho. In the map area, the Wasatch fault system consists of the north–northwest-striking Clarkston Mountain and Malad City segments, originally defined by Machette et al. (1992). Throw on the Malad City segment is estimated by Zoback (1983) to be 2.56 km just to the north of the study area. Machette et al. (1992) found no evidence for post-Lake Bonneville activity on these two segments of the fault, and infer latest activity in the Late Pleistocene. The Clarkston Mountain segment terminates near a shallowly buried bedrock ridge in the middle of Malad Valley, as interpreted from gravity data (Zoback, 1983; Eversaul, 2004).

The presence of a segment boundary in the study area was documented by Machette et al. (1992) and was originally described as a complexly faulted bedrock salient. However, we reinterpret the geometry of this boundary as a faulted relay ramp formed from a 2.5–3.5-km-wide en echelon right step between the two fault segments. This is based on map data indicating the continuation of the Malad City segment into the Malad Range, which shows a northward increase in displacement (Fig. 3) (Long, 2004; Long et al., 2004).

Late Cenozoic Extensional Folding

Several folds deform the Salt Lake Formation in the study area at a variety of scales and attitudes (Fig. 3). These folds are interpreted as extensional in origin, similar to those documented by Janecke et al. (1998), because no contractional faults are present in the study area. Collectively, these folds are interpreted as the result of internal hanging-wall deformation that accompanied normal faulting, with most folds interpreted as rollover anticlines that formed above listric faults of Late Miocene or Pliocene–Quaternary age. In the southern half of the study area, the folds collectively form a north–northwest-trending, faulted antiformal accommodation zone, using the terminology of Faulds and Varga (1998). This antiform is represented by the Jenkins Hollow anticline in the southern end of the map area (Fig. 3), but consists of two parallel anticlines with an intervening faulted syncline further to the north. The antiform is cut by several small-offset normal faults, which may be indicative of rollover anticline crestal collapse, but spatial and temporal relationships between the folds and faults are unresolved. The inward-dipping Late Miocene Steel Canyon and Pliocene–Quaternary Deep Creek faults bound the east and west sides of the antiformal zone, and are interpreted as listric at depth. Together, these two faults of differing age probably produced the antiformal fold system as a complex double-rollover anticline in multiple phases of Late Cenozoic extension. However, this interpretation is complicated by the fact that similar dip domains in their hanging walls persist into the footwalls of both structures. It is also possible that the western limb of this anticline is still growing due to westward tilting above an east-dipping structure buried along the west edge of Malad Valley. Gravity studies suggest a large east-dipping normal fault on the western margin of Malad Valley (Zoback, 1983; Eversaul, 2004), which may have steepened the dip of the west limb of the antiform over time.

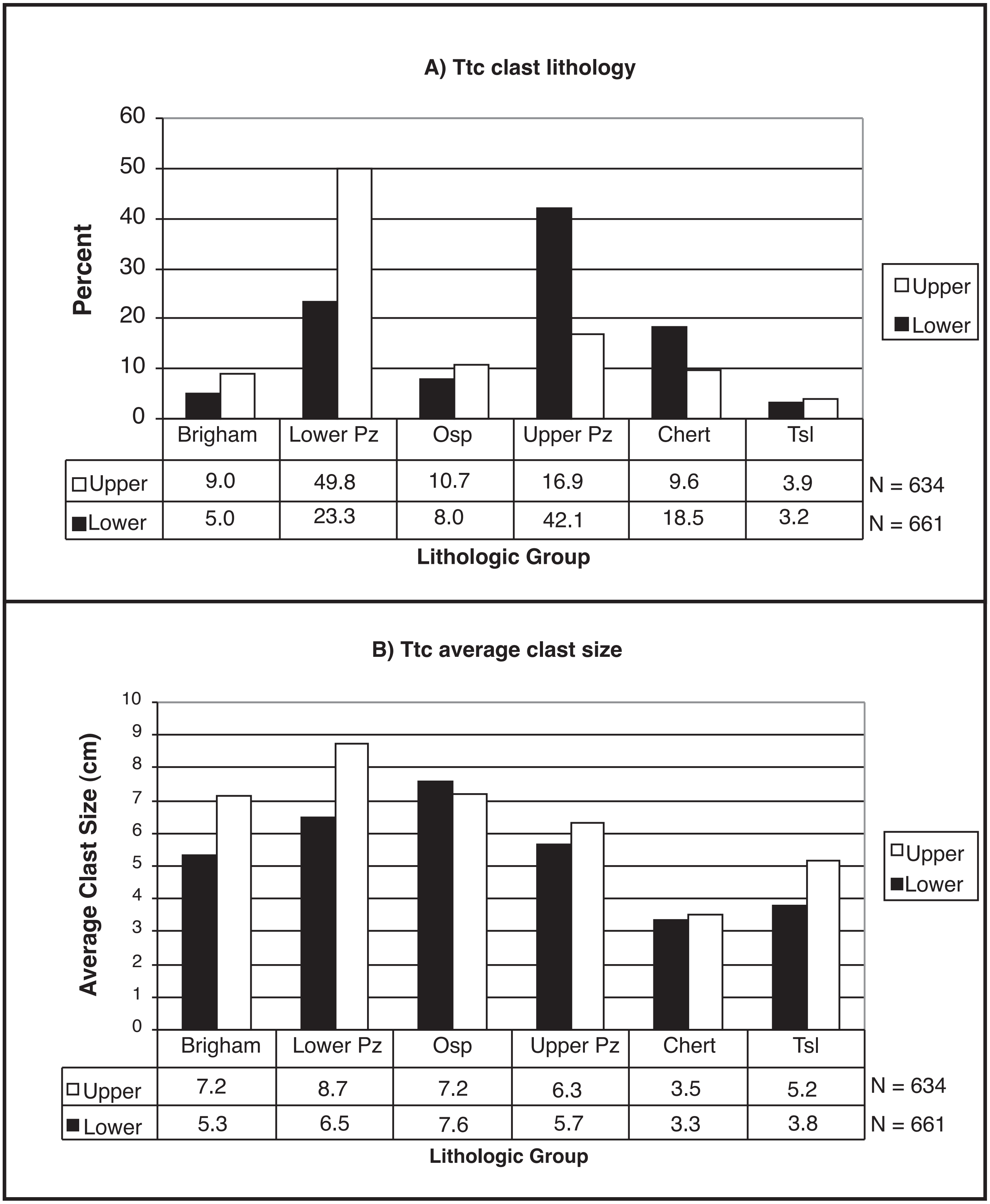

Figure 9. Histograms showing: ***A***, clast lithology, and ***B***, average clast size, for lower and upper parts of the section of the Third Creek Member (Ttc) of the Salt Lake Formation. Note that both the number and average size of Lower Paleozoic and Brigham Group clasts increase upsection. Charts modified from Long (2004).

DISCUSSION

Interpretation of Extension and Basin Development

Paleocene–Eocene (?) Wasatch Formation

In the study area, the Wasatch (?) Formation is interpreted to record an episode of north–south extension of Paleocene–Eocene (?) and older age. The Willow Spring fault is interpreted to be syntectonic with Wasatch (?) Formation deposition. As slip along this structure initiated, an east-striking Paleocene–Eocene (?) half-graben was formed and the conglomerate unit was deposited in its hanging wall (Fig. 10*A*). Silurian and Devonian units were eroded off of the footwall during deposition, and were presumably transported to the north, where they are preserved as clasts in the Wasatch conglomerate. The presence of externally derived Upper Paleozoic or Mesozoic clasts indicates that the conglomerate was probably deposited by an east- or west-flowing stream system.

As the Willow Spring fault continued to slip, units in its footwall eroded to the level of the Ordovician Swan Peak quartzite. This unit served as the main source for clasts of the Wasatch Formation boulder beds, which were transported, likely by debris flows, to the north as a coarse fan gravel (Fig. 10*B*). At the end of slip and deposition, a few thin beds of the boulder unit were deposited across the Willow Spring fault and its footwall. This is consistent with studies to the south of the map area, where the formation consists of a thin, coarse, unconsolidated rubble sheet, dominated by Paleozoic quartzite clasts (Biek et al., 2003).

Skyline Member

The Middle to Late Miocene Skyline Member of the Salt Lake Formation was deposited in a north-striking three-dimensional half-graben, here named the Skyline subbasin, in the north half of the study area. This basin was bounded on the east by the west-dipping Red Knoll and Trespass syntectonic normal faults, and on the south by the north-dipping Spring Trail syntectonic normal fault (Fig. 10*C*). Thickness relationships between the Skyline Member and these structures provide evidence for an isolated extensional event as old as 11.93 Ma, which predates slip on the Bannock detachment system (Janecke et al., 2003). The unit was deposited as an alluvial apron composed of coarse-grained, locally sourced Cambrian–Devonian clasts. The Skyline Member also contains detrital zircons that may have been derived from a stream that drained the Owyhee–Humboldt volcanic field in southwest Idaho (Link et al., 1999, 2005; Beranek, 2005).

Overall, the Skyline subbasin has an estimated north–south length of ~11 km, based on the extent of the Red Knoll growth fault within (Long, 2004) and north of the map area (Janecke and Evans, 1999; Janecke et al., 2003). The southern end of this basin coincides with the east-striking Spring Trail fault, which truncates against the Red Knoll fault on its east end. This structure forms a square-shaped southern end to the basin (in map view), and eliminates most of the section of the Skyline Member in its footwall. The Spring Trail fault may have a significant component of strike-slip, due to its orthogonal strike to the Red Knoll fault, but no kinematic indicators were found to support this hypothesis. The Spring Trail fault merges with the Willow Spring fault on its west end, which indicates that the two structures may be

Figure 10, (p.20–22). Block diagrams representing the map area during the: ***A(p. 20)***, Paleocene–Eocene (?), shows deposition of Wasatch (?) Formation fluvial conglomerate unit (Twc) in an east-striking half-graben formed form slip on the Willow Spring fault. ***B(p. 20)***, Paleocene–Eocene (?), after the events in Figure 10*A*. Shows boulder unit of the Wasatch (?) Formation (Twb) deposited as fan gravel on both sides of Willow Spring fault. Note that both units of Wasatch (?) Formation thicken toward Willow Spring fault. ***C(p. 21)***, Middle to Late Miocene (~11.9–10.2 Ma), prior to slip on Bannock detachment system. Skyline subbasin forms from slip on Red Knoll, Trespass, and Spring Trail faults; Skyline Member (Ts) deposited as alluvial fans. Lower conglomerate unit (Tscl) deposited in a shallow basin to south, possibly by east-flowing streams. ***D(p. 21)***, Late Miocene (~10.2–<9.2 Ma), during slip on Bannock detachment system. An uplifted fault block forms within the lacustrine basin of the Cache Valley Member (Tcv) from slip on the Steel Canyon fault. Tcv deposited as tufa near lake margin, and as micrite further out into lake. Third Creek Member (Ttc) deposited as alluvial fan in proximity to active Steel Canyon fault. Rollover adjacent to Steel Canyon fault forms west limb of complex antiformal zone of extensional folds. ***E(p.22)***, Pliocene–Quaternary; two segments of the Wasatch fault accommodate uplift of Malad Range and subsidence of Malad Valley, which fills with synextensional deposits (Qu). The two segments are linked by a right-step, which forms a faulted relay ramp. Rollover adjacent to Deep Creek fault forms eastern limb of antiformal zone of extensional folds. Lake Bonneville was present in Malad Valley in the Holocene. All block diagrams modified from Long (2004).

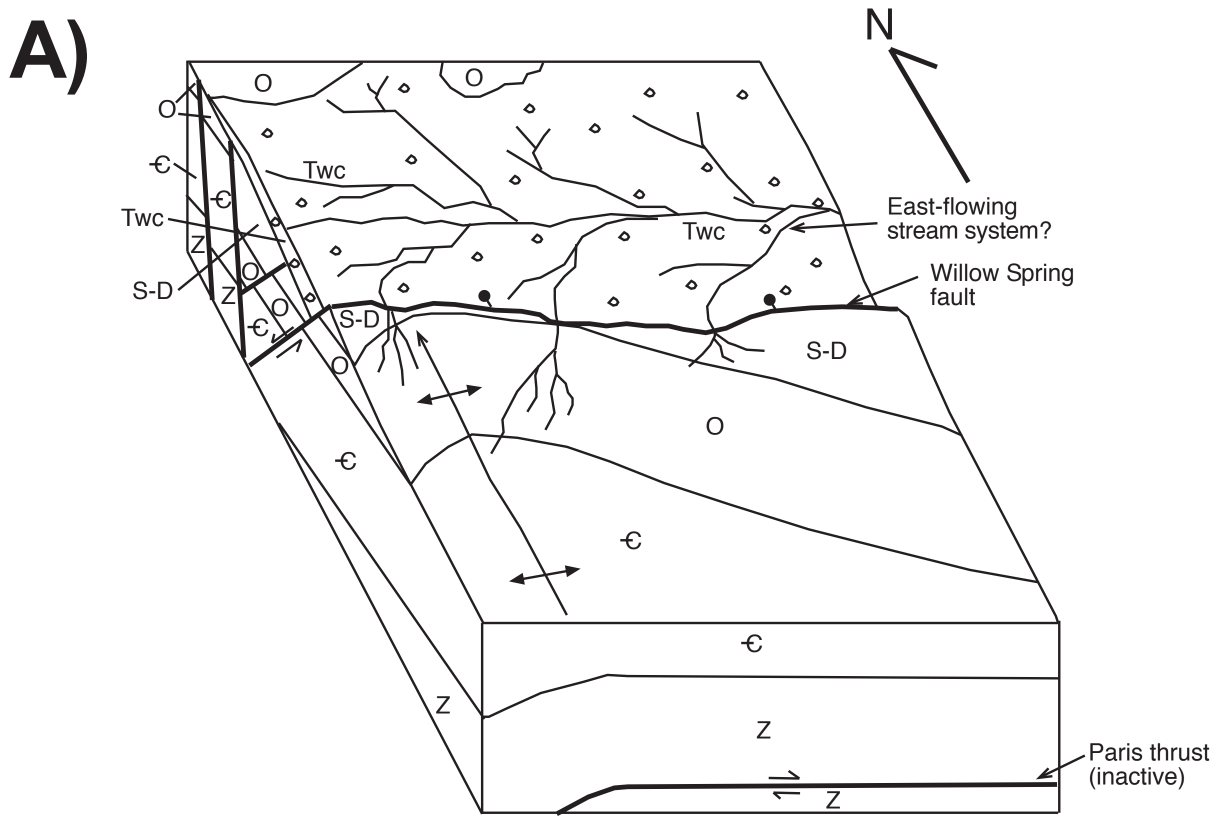
A)
N
O
O
O
Є
Twc
Twc
Є
Z
S-D
Z
O
O
Є
S-D
O
Twc
East-flowing
stream system?
Willow Spring
fault
S-D
O
Є
Є
Є
Z
Z
Paris thrust
(inactive)
Z

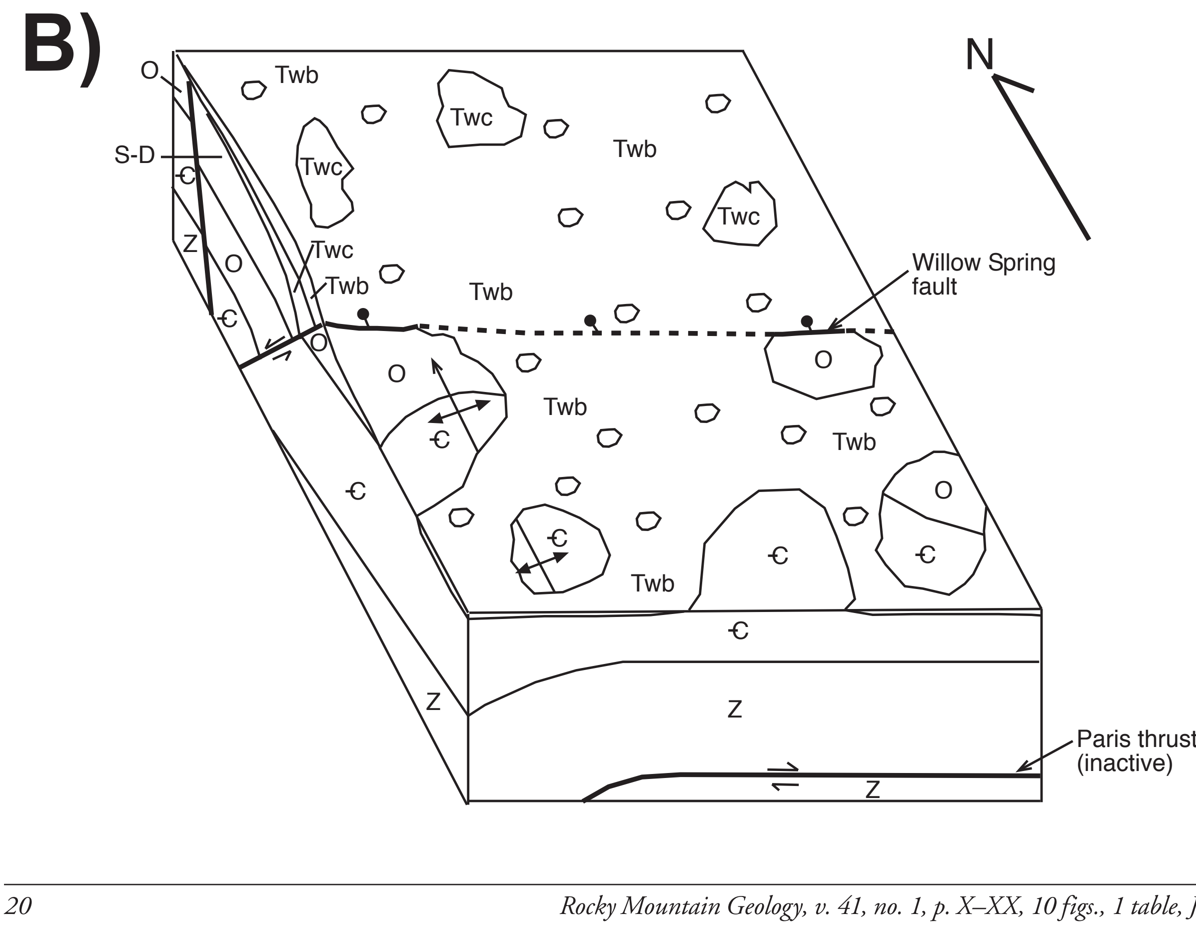
B)
N
O
Twb
Twc
S-D
Twc
Є
Twb
Twc
Z
O
Twc
Twb
Є
Twb
Twb
Willow Spring
fault
O
O
O
Twb
Є
Twb
Є
O
Є
Є
Є
Twb
Є
Z
Z
Paris thrust
(inactive)
Z

C)

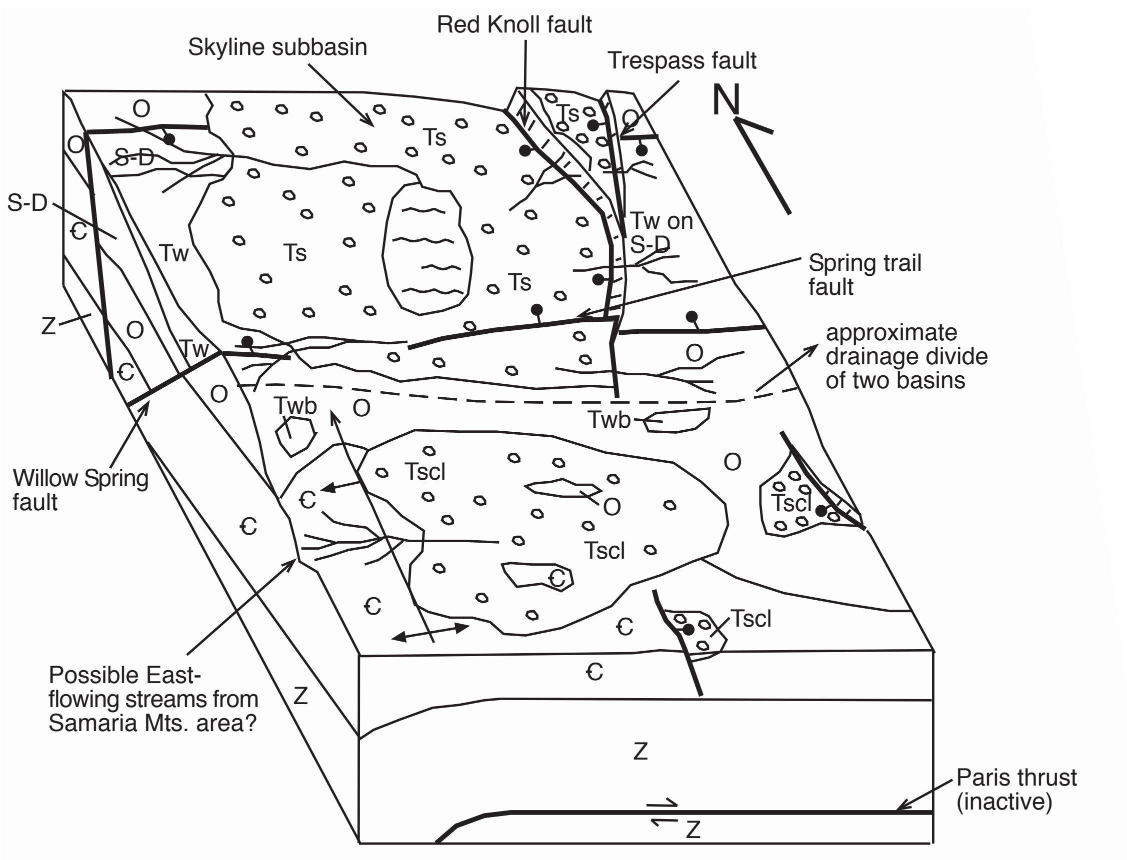
Red Knoll fault
Skyline subbasin
Trespass fault
N
O
Ts
O
S-D
Ts
S-D
Є
Tw
Ts
Ts
Tw on
S-D
Spring trail
fault
Z
O
Tw
Є
O
approximate
drainage divide
of two basins
Twb
O
Twb
Willow Spring
fault
Tscl
O
Є
Tscl
O
Є
Tscl
Є
Є
Tscl
Є
Possible East-
flowing streams from
Samaria Mts. area?
Z
Z
Paris thrust
(inactive)
Z

D)

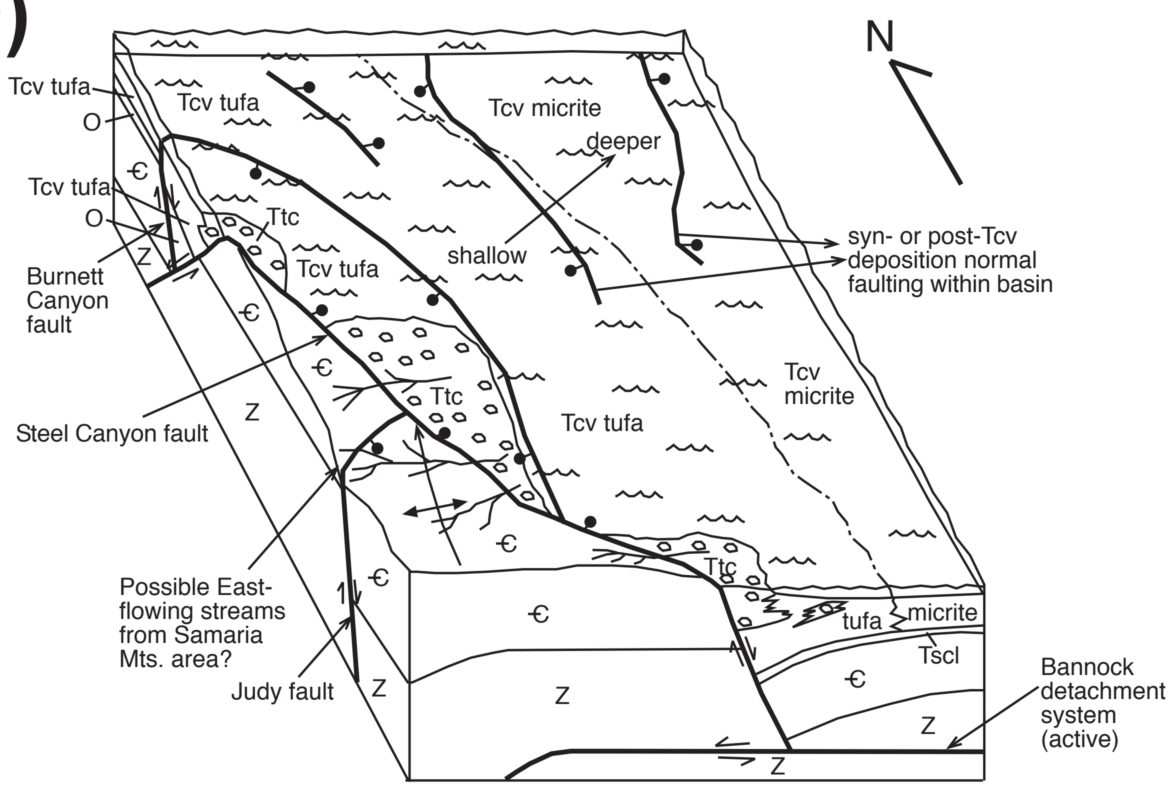
N
Tcv tufa
Tcv tufa
O
Tcv micrite
deeper
Є
Tcv tufa
O
Ttc
Z
shallow
Tcv tufa
syn- or post-Tcv
deposition normal
faulting within basin
Burnett
Canyon
fault
Є
Є
Tcv
micrite
Steel Canyon fault
Z
Ttc
Tcv tufa
Є
Possible East-
flowing streams
from Samaria
Mts. area?
Є
Ttc
Є
tufa
micrite
Tscl
Є
Judy fault
Z
Z
Z
Bannock
detachment
system
(active)
Z

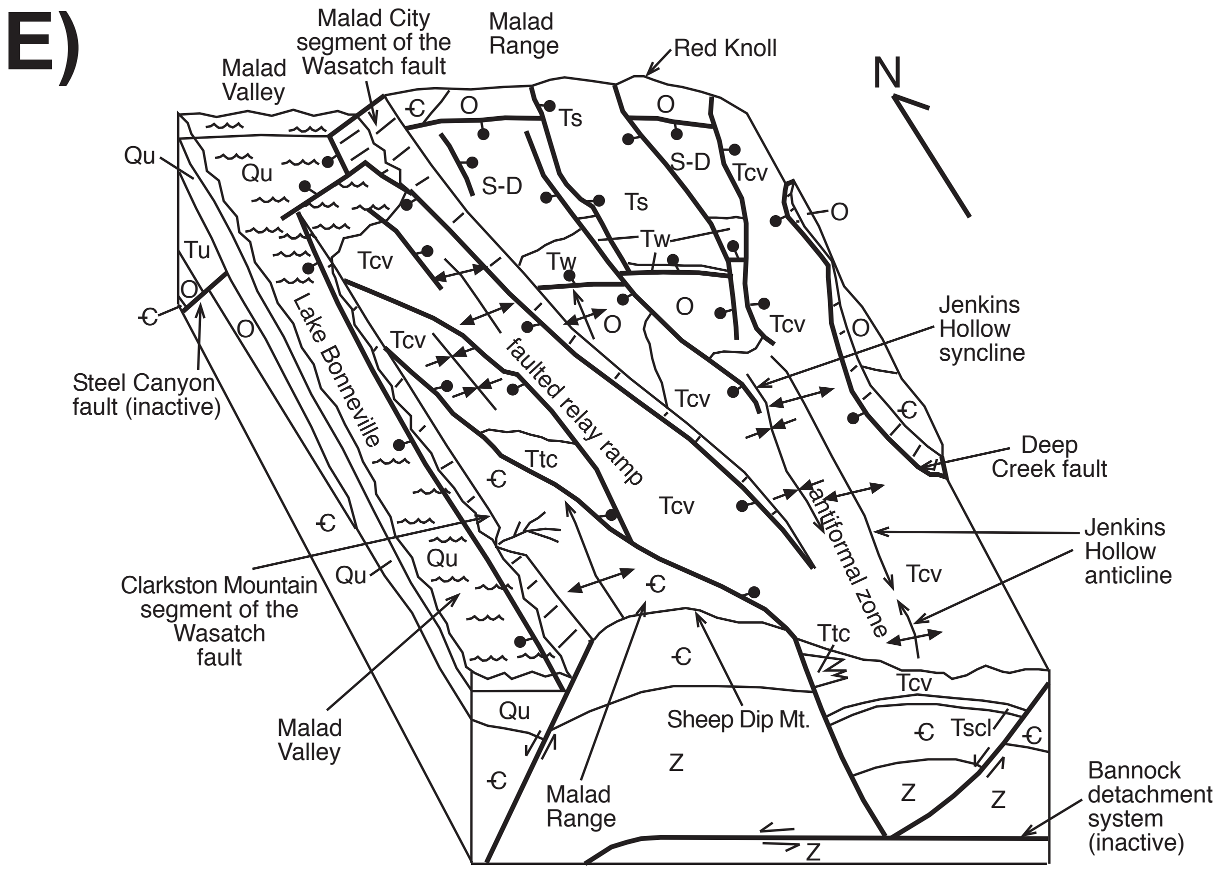

connected at depth, and that the Spring Trail fault probably represents a Miocene reactivation of part of the Paleocene–Eocene (?) structure.

Lower conglomerate unit

The lower conglomerate unit of the Salt Lake Formation represents a basal conglomerate that filled pre-existing topographic lows, based on significant thickness variations seen at its few exposures, and abrupt pinch-outs over short distances. A local high percentage of Upper Paleozoic clasts indicates that the conglomerate may have had a partial source from the Samaria Mountains area to the west, which contains the closest exposures of Upper Paleozoic rocks (Platt, 1977). Therefore, the conglomerate may have been deposited by east-flowing streams (Fig. 9*C*).

Cache Valley Member

In the Henderson Creek Quadrangle, the Cache Valley Member of the Salt Lake Formation contains a tufa-rich lake-margin facies that interfingers with coarse basin-margin deposits of the Third Creek Member. The lacustrine system was active from ~10.2 Ma to at least ~9.2 Ma. The Steel Canyon fault began to slip by at least ~10 Ma and formed a local highland within the lacustrine basin (Fig. 10*D*). Adjacent to the Steel Canyon fault, the tufa-rich facies of the Cache Valley Member was deposited in a shallow, freshwater lake-margin setting. To the north of the map area, the lake underwent a saline-alkaline phase during this time period, which produced zeolites in tuffaceous beds (Carney, 2002; Janecke et al., 2003). However, deposits in a single lake can range from freshwater to hypersaline, just as they can range from carbonate- to siliciclastic-rich, with variable tectonic influences (Carroll and Bohacs, 1999). Also, it is possible that the inflow of fresh water from streams into the lake kept water fresh along the margins, while conditions in the interior of the lake remained saline. Northeast of the lake-margin facies, the micrite and tuffaceous siltstone-rich facies of the Cache Valley Member was deposited in a more distal part of the lake than the tufa (Fig. 10*D*), and farther east, altered tuffaceous beds in the Weston Canyon quadrangle may represent the interior of the Cache Valley Member lake (Steely et al., 2005). The lake may have become deeper to the northeast, away from the Steel Canyon fault, which is compatible with the open lacustrine setting interpretation (Janecke et al., 2003).

Third Creek Member

The Third Creek Member of the Salt Lake Formation was deposited as a localized clastic wedge, with a source in the footwall of the active Steel Canyon fault (Fig. 10*D*). This structure probably formed an intrabasinal high within the lake system, based on the regional distribution of Cache Valley Member deposits and the presence of the Third Creek Member along only a fraction of the fault's length. The ~10.0–<9.2-Ma age of the member indicates that deposition was coeval with the upper part of the Cache Valley Member section. The base of the Third Creek Member section is interpreted as beach or stream deposits, due to a high percentage of rounded and weathered Upper Paleozoic clasts. These may have been brought in from a stream system sourced from the Samaria Mountains area to the west, which contains Upper Paleozoic rocks (Platt, 1977) (Fig. 10*D*). The upper section of the Third Creek Member is interpreted as an alluvial fan deposit, shed from the footwall highlands of the Steel Canyon fault. An upsection increase in the number and average size of Lower Paleozoic and Brigham Group clasts indicates the unroofing of the footwall of the Steel Canyon fault.

Extensional folding and Pliocene–Quaternary faulting

The hanging wall section east of the Steel Canyon fault was complexly folded and faulted into a broad antiformal zone as a result of separate Late Miocene and Pliocene–Quaternary episodes of extensional faulting. The Jenkins Hollow anticline and associated north–northwest-trending folds were formed from rollover and internal hanging wall deformation above the Late Miocene Steel Canyon fault and the Pliocene–Quaternary Deep Creek fault (Figs. 10*D* and *E*). It is possible that this antiform was affected by deformation within the relay ramp between the stepping segments of the Pliocene–Quaternary Wasatch fault, and that its west limb was steepened by a fault within Malad Valley. The segments of the Wasatch fault accommodated relative uplift of the Malad Range and subsidence of Malad Valley (Fig. 10*E*).

IMPLICATIONS

Interpretations made in this project have several implications for our understanding of the complex structural and tectonic development of the northeast margin of the Basin and Range province. Prior to this study, it was suggested that the Bannock detachment system represents Miocene and younger, low-angle, high-magnitude extension in this part of the Basin and Range province followed by low-magnitude extension along the currently active Wasatch and West Cache fault zones (Janecke and Evans, 1999; Carney, 2002; Janecke et al., 2003). Our study furthers understanding of this detachment system, through analyzing deformation and syntectonic deposition in its hanging wall, and more clearly separating pre- and post-detachment faulting episodes of extension. Hanging-wall features that we recognized, including synthetic and antithetic faults, complex zones of extensional folds that formed sequentially, and the amount of internal extension, all have implications for the evolution of the upper blocks of low-angle fault systems with progressive extension. Dating of the wedge of conglomerate shed into the lacustrine basin from the footwall block of the large Steel Canyon antithetic normal fault shows that the hanging wall of the Bannock detachment fault began to break up very early in its history, perhaps as little as 0.2 million years after its inception.

In addition to detachment-related implications, our study shows that extension began in the region in the Paleocene–Eocene (?), and was followed by three episodes of late Cenozoic east–west extension. Our study expands the area of documented Paleocene–Eocene (?) extension, but shows that it was directed north–south, rather than east–west, as interpreted in the next mountain range to the east (Oaks and Runnells, 1992). We show that a graben-forming extensional event during deposition of the Skyline Member of the Salt Lake Formation predated slip on the Bannock detachment system, and produced a rectangular half-graben in plan view due to reactivation of a north-dipping Paleocene–Eocene (?) normal fault at its south end. Finally, the detrital zircon data that suggest ~10-Ma eastward transportation of grains from volcanic fields in southwest Idaho are consistent with previous studies (Link et al., 1999, 2005; Beranek, 2005) about the development of drainage systems in southern Idaho during northeast passage of the Yellowstone hot spot.

CONCLUSIONS

The Malad Range of southern Idaho and northern Utah experienced four distinct episodes of Cenozoic extension, each of which was accompanied by synextensional sedimentation. A Paleocene–Eocene (?) and older set of east-striking normal faults is interpreted to be associated with deposition of the Wasatch (?) Formation, a conglomeratic- and boulder-rich unit deposited in a south-tilted half-graben formed by from slip on the Willow Spring fault.

Starting at ~12 Ma, Middle and Late Miocene north–northwest-striking normal faults formed in two distinct events recorded by synextensional strata of the Salt Lake Formation. The 11.9–10.2-Ma Skyline Member predates slip on the Bannock detachment system and was deposited as alluvial fans in a three-dimensional, east-tilted half-graben bound by the Red Knoll, Trespass, and Spring Trail syntectonic normal faults. The second and more extensive Late Miocene extensional event is associated with slip and subsequent breakup of the hanging wall of the regional Bannock detachment system. The 10.2–<9.2-Ma Cache Valley Member consists of carbonate and tuffaceous deposits of a lake system that formed in a regionally continuous basin above the detachment (Janecke and Evans, 1999; Carney, 2002; Janecke et al, 2003; Carney and Janecke, 2005). The 10.0–<9.2-Ma Third Creek Member, which interfingers with the lacustrine deposits, represents a coarse clastic wedge which was sourced from the footwall of the intrabasinal Steel Canyon syntectonic normal fault.

The most recent stage of extension in the study area involved Pliocene–Quaternary normal faulting. The active Wasatch fault is the largest structure associated with this event and consists of two right-stepping segments separated by a faulted relay ramp. This differs from a previous interpretation as a bedrock salient (Machette et al., 1992). Extensional folds identified in Miocene deposits in the map area form a broad, complexly faulted antiformal zone, and are interpreted as the result of double-rollover above two oppositely dipping listric structures of different age, the Late Miocene Steel Canyon fault and the Pliocene–Quaternary Deep Creek fault.

ACKNOWLEDGMENTS

We thank the USGS EDMAP program, grant 03HQAG0118, through which this project was partially funded. Detrital zircon analyses and tephra correlations were supported by NSF EAR 0125756 to Paul K. Link. We would also like to thank David W. Rodgers of Idaho State University, James E. Faulds of the Nevada Bureau of Mines and Geology (Reno), and Michael L. Wells of University of Nevada, Las Vegas, for reviews of this manuscript.

REFERENCES CITED

Allmendinger, R. W., 1982, Sequence of late Cenozoic deformation in the Blackfoot Mountains, southeastern Idaho, *in* Bonnichsen B. and Breckenridge R. M., eds., Cenozoic Geology of Idaho: Idaho Bureau of Mines and Geology Bulletin 26, p. 505–516.

______1992, Fold and thrust tectonics of the western United States exclusive of the accreted terranes, *in* Burchfiel, B. C., Lipman, P. W., and Zoback, M. L., eds., The Cordilleran Orogen: Conterminous U.S.: Boulder, Colorado, Geological Society of America, The Geology of North America, v. G-3, p. 583–608.

Armstrong, F. C., and Oriel, S. S., 1965, Tectonic development of the Idaho–Wyoming thrust belt: American Association of Petroleum Geologists Bulletin, v. 49, p. 1847–1866.

Axtell, D. C., 1967, Geology of the northern part of the Malad Range, Idaho [M.S. thesis]: Logan, Utah State University, 65 p.

Beranek, L. P., 2005, Shrimp U-Pb detrital zircon geochronology of Miocene to Holocene sediments in the Snake River Plain region: tracking eastward migration of the Yellowstone hotspot [M.S. thesis]: Pocatello, Idaho State University, 170 p.

Biek, R. F., Oaks, R. Q., Jr., Janecke, S. U., Solomon, B. J., and Swenson, B. L. M., 2003, Geologic maps of the Clarkston and Portage quadrangles, Box Elder and Cache Counties, Utah, and Franklin and Oneida Counties, Idaho: Utah Geological Survey Map 194, scale 1:24,000, 3 sheets, with 41-p. pamphlet.

Bryant, B., 1990, Geologic map of the Salt Lake City 30' x 60' Quadrangle, north-central Utah, and Uinta County, Wyoming: U.S. Geological Survey Miscellaneous Investigations Series Map I-1944, scale 1:100,000, 1 sheet.

Carney, S. M., 2002, Evolution of a Miocene–Pliocene low-angle normal fault system in the southern Bannock Range, southeast Idaho [M.S. thesis]: Logan, Utah State University, 170 p.

Carney, S. M., and Janecke, S. U., 2005, Excision and the original low dip of the Miocene–Pliocene Bannock detachment system, SE Idaho: Northern cousin of the Sevier Desert detachment?: Geological Society of America Bulletin, v. 117, p. 334–353.

Carney, S. M., Janecke, S. U., Oriel, S. S., Evans, J. C., and Link, P. K., 2002, Geologic map of the Clifton quadrangle, Franklin and Oneida Counties, Idaho: Idaho Geological Survey Technical Report T-03-4, scale 1:24,000, 2 sheets.

Carroll, A. R., and Bohacs, K. M., 1999, Stratigraphic classification of ancient lakes: Balancing tectonic and climatic controls: Geology, v. 27, p. 99–102.

Compston, W., Williams, I. S., Kirschvink, J. L., Zhang, Z., and Ma, G., 1992, Zircon U-Pb ages for the Early Cambrian time-scale: Journal of the Geological Society London, v. 149, p. 171–184.

Coogan, J. C., 1992, Structural evolution of piggyback basins in the Wyoming–Idaho–Utah thrust belt, *in* Link, P. K., Kuntz, M. A., and Platt, L. B., eds., Regional geology of eastern Idaho and western Wyoming: Boulder, Colorado, Geological Society of America Memoir 179, p. 55–82.

Crane, T. C., 2000, Geologic mapping and gravity survey of the Lava Hot Springs, Idaho, 7.5 min. quadrangle: Evidence for a Late Miocene supradetachment basin in Southeast Idaho [M.S. thesis]: Pocatello, Idaho State University, 147 p.

Danzl, R. B., 1982, Stratigraphy and depositional environment of the Tertiary Salt Lake Group near Oneida Narrows, southeastern Idaho: Northwest Geology, v. 11, p. 22–30.

______1985, Depositional and diagenetic environment of the Tertiary Salt Lake Group at Oneida Narrows, southeastern Idaho [M.S. thesis]: Pocatello, Idaho State University, 177 p.

DeCelles, P. G., 1994, Late Cretaceous–Paleocene synorogenic sedimentation and kinematic history of the Sevier thrust belt, northeast Utah and southwest Wyoming: Geological Society of America Bulletin, v. 106, p. 32–56.

DeVecchio, D., 2002, Geologic mapping of the Downey East quadrangle and regions of the Swan Lake, Oxford, and Cottonwood Peak quadrangles, Bannock County, Idaho: Multiple phases of Miocene to Quaternary extensional tectonics [M.S. thesis]: Pocatello, Idaho State University, 103 p.

Eversaul, M. L., 2004, Basin structure of proposed Late Miocene to Pliocene supradetachment basins in SE Idaho, based on detailed gravity and geologic data [M.S. thesis]: Pocatello, Idaho State University, 132 p.

Faulds, J. E., and Varga, R. J., 1998, The role of accommodation zones and transfer zones in the regional segmentation of extended terranes, *in* Faulds, J. E., and Stewart, J. H., eds., Accommodation zones and transfer zones: The regional segmentation of the Basin and Range Province: Boulder, Colorado, Geological Society of America Special Paper 323, p. 1–45.

Ford, T. D., and Pedley H. M., 1996, A review of tufa and travertine deposits of the world: Earth-Science Reviews 41, p. 117–175.

Goessel, K. M., Oaks, R. Q., Jr., Perkins, M. E., and Janecke, S. U., 1999, Tertiary stratigraphy and structural geology, Wellsville Mountains to Junction Hills, north-central Utah, *in* Spangler, L., and Allen, C., eds., Geology of northern Utah and vicinity: Utah Geological Association Publication 27, p. 45–69.

Hayden, F. V., 1869, Preliminary field report [third annual] of the United States Geological Survey of Colorado and New Mexico: 155 p.

Jacobson, S. R., and Nichols, D. J., 1982, Palynological dating of syntectonic units in the Utah–Wyoming thrust belt; the Evanston Formation, Echo Canyon Conglomerate, and Little Muddy Creek Conglomerate, *in* Powers, R. B., ed., Geologic studies of the Cordilleran thrust belt: Rocky Mountain Association of Geologists Symposium, Denver, Colorado, 1982, v. 1, p. 735–750.

Janecke, S. U., and Evans, J. C., 1999, Folded and faulted Salt Lake Formation above the Miocene to Pliocene New Canyon and Clifton detachment faults, Malad and Bannock Ranges, Idaho, field trip guide to the Deep Creek half-graben and environs: *in* Hughes, S. S., and Thackray, G. D., eds., Guidebook to the geology of eastern Idaho: Idaho Museum of Natural History, Pocatello, Idaho, p. 71–96.

Janecke, S. U., Carney, S. M., Perkins, M. E., Evans, J. C., Link, P. K., Oaks, R. Q., Jr., and Nash, B. P., 2003, Late Miocene–Pliocene detachment faulting and Pliocene–Pleistocene Basin and Range extension inferred from dismembered rift basins of the Salt Lake Formation, southeast Idaho; *in* Raynolds, R., and Flores, R., eds., Cenozoic systems of the Rocky Mountain Region: Denver, Colorado, Rocky Mountain Section SEPM (Society for Sedimentary Geology), p. 369–406.

Janecke, S. U., Vandenburg, C. J., and Blankenau, J. J., 1998, Geometry, mechanisms and significance of extensional folds from examples in the Rocky Mountain Basin and Range province, U.S.A.: Journal of Structural Geology, v. 20, p. 841–856.

Kruger, J. M., Crane, T. J., Pope, A. D., Perkins, M. E., and Link, P. K., 2003, Structural and stratigraphic development of Neogene basins in the Marsh Valley, Lava Hot Springs, and Wakley Peak areas, southeast Idaho: Two phases of extension; *in* Raynolds, R., and Flores, R., eds., Cenozoic systems of the Rocky Mountain region: Denver, Colorado, Rocky Mountain Section SEPM (Society for Sedimentary Geology), p.1–51.

Lamerson, P. R., 1982, The Fossil Basin and its relationship to the Absaroka thrust system, Wyoming and Utah, *in* Powers, R. B., ed., Geologic studies of the Cordilleran thrust belt: Denver, Colorado, Rocky Mountain Association of Geologists Symposium, v. 1, p. 279–340.

Link, P. K., 1982a, Geology of the Upper Proterozoic Pocatello Formation, Bannock Range, southeastern Idaho [Ph.D. dissert.]: University of California, Santa Barbara, 131 p.

______1982b, Structural geology of the Oxford and Malad Summit quadrangles, Bannock Range, southeastern Idaho, *in* Powers, R. B., ed., Geologic studies of the Cordilleran thrust belt: Denver, Colorado, Rocky Mountain Association of Geologists, v. 2, p. 851–858.

Link, P. K., and Stanford, L. R., 1999, Geologic map compilation of the Pocatello 30 x 60 minute quadrangle, Idaho: Idaho Geological Survey Technical Report 99-2, scale 1:100,000, 1 sheet.

Link. P. K., Fanning. C. M., and Beranek, L. P, 2005, Reliability and longitudinal change of detrital-zircon age spectra in the Snake River system, Idaho and Wyoming: An example of reproducing the bumpy barcode: Sedimentary Geology, v. 182, p. 101–142.

Link, P. K., Reading, R. W., Godfrey, A. E., and Prevedel, D., 1999, Topographic development of the Snake River Plain, Idaho, *in* Hughes, S.S., and Thackray, G.D., eds., Guidebook to the geology of eastern Idaho: Pocatello, Idaho Museum of Natural History, back cover.

Long, S. P., 2004, Geology of the Henderson Creek quadrangle, Oneida County, Idaho: Multiple phases of Tertiary extension and deposition [M.S. thesis]: Pocatello, Idaho State University, 158 p.

Long, S. P., Link, P. K., Janecke, S. U., and Rodgers, D. W., 2004, Geologic Map of the Henderson Creek quadrangle, Oneida County, Idaho. Idaho Geological Survey Technical Report T-04-3, 1:24,000-scale, 1 sheet.

Ludwig, K. R., 2003, Isoplot/Ex version 3.0.: A geochronological toolkit for Microsoft Excel: Berkeley Geochronology Center Special Publication No. 1a, 2455 Ridge Road, Berkeley CA 94709, USA.

Machette, M. N., Personius, S. F., and Nelson, A. R., 1992, Paleoseismology of the Wasatch fault zone—A summary of recent investigations, interpretations, and conclusions: U.S. Geological Survey Professional Paper 1500A, p. A1–A71.

Mansfield, G. R., 1920, The Wasatch and Salt Lake formations of southeastern Idaho: American Journal of Science, v. 49, p. 399–406.

______1927, Geography, geology, and mineral resources of the Fort Hall Indian Reservation, Idaho: U.S. Geological Survey Professional Paper 319, 453 p.

Miller, D. M., 1991, Mesozoic and Cenozoic tectonic evolution of the northeastern Great Basin, *in* Buff, R. H., and Coyner, A. R., eds., Geology and ore deposits of the Great Basin: Geological Society of Nevada, Field Guidebook Compendium, v. 1, p. 202–228.

Morgan, L. A., and McIntosh, W. C., 2005, Timing and development of the Heise volcanic field, Snake River Plain, Idaho, western USA; Geological Society of America Bulletin, v. 117, p. 288–306.

Oaks, R. Q., Jr., Smith, K. A., Janecke, S. U., Perkins, M. E., Nash, W. P., 1999, Stratigraphy and tectonics of Tertiary strata of southern Cache Valley, north-central Utah, *in* Spangler, L., and Allen, C., eds., Geology of northern Utah and vicinity: Utah Geological Association Publication 27, p. 45–69.

Oaks, R. Q., Jr., and Runnells, T. R., 1992, The Wasatch Formation in the central Bear River Range, northern Utah: Utah Geological Survey Contract Report 92-8, 79 p.

Ore, H. T., 1982, Geologic field guide to Tertiary-Quaternary sediments in the Pocatello Region: Northwest Geology, v. 11, p. 47–55.

Oriel, S. S., and Tracey, J. I., 1970, Uppermost Cretaceous and Tertiary stratigraphy of Fossil Basin, southwestern Wyoming: U.S. Geological Survey Professional Paper 635, 53 p.

Oriel, S. S., and Platt, L. B., 1980, Geologic map of the Preston 1ºx2º quadrangle, Idaho and Wyoming: U.S. Geological Survey Miscellaneous Investigations Series Map I-1127, scale 1:250,000, 1 sheet.

______1979, Younger-over-older thrust plates in southeastern Idaho: Geological Society of America Abstracts with Programs, v. 11, no. 6, p. 298.

Perkins, M. E., Brown, F. H., Nash, W. P., McIntosh, W., and Williams, S. K., 1998, Sequence, age, and source of silicic fallout tuffs in middle to late Miocene basins of the northern Basin and Range province: Geological Society of America Bulletin, v. 110, p. 344–360.

Perkins, M. E., Nash, W. P., Brown, F. H., and Fleck, R. J., 1995, Fallout tuffs of Trapper Creek, Idaho—A record of Miocene explosive volcanism in the Snake River Plain volcanic province: Geological Society of America Bulletin, v. 107, p. 1484–1506.

Perkins, M. E., and Nash, W. P., 2002, Explosive silicic volcanism of the Yellowstone hotspot: the ash-fall tuff record: Geological Society of America Bulletin, v. 114, p. 367–381.

Pierce, K. L., and Morgan, L. A., 1992, The track of the Yellowstone hotspot; volcanism, faulting, and uplift, *in* Link, P. K., Kuntz, M. A., and Platt, L. B., eds., Regional geology of eastern Idaho and western Wyoming: Geological Society of America Memoir 179, p. 1–53.

Platt, L. B., 1977, Geologic Map of the Ireland Springs–Samaria area, southeastern Idaho and northern Utah: United States Geological Survey Miscellaneous Field Studies Map MF-890, scale 1:48,000, 1 sheet.

Pope, A. D., Blair, J. J., and Link, P. K., 2001, Geologic Map of the Wakley Peak quadrangle, Idaho: Idaho Geological Survey Technical Report T-01-4, scale 1:24,000, 1 sheet.

Rodgers, D. W., and Janecke, S. U., 1992, Tertiary paleogeologic maps of the western Idaho–Wyoming–Montana thrust belt, *in* Link, P. K., Kuntz, M. A., and Platt, L. B., eds., Regional geology of eastern Idaho and western Wyoming: Boulder, Colorado, Geological Society of America Memoir 179, p. 83–94.

Rodgers, D. W., Ore, H. T., Bobo, R. T., McQuarrie, N., and Zentner, N., 2002, Extension and subsidence of the eastern Snake River Plain, Idaho, *in* Bonnichsen, B., White, C. M., and McCurry, M., eds., Tectonics and magmatic evolution of the Snake River Plain volcanic province: Idaho Geological Survey Bulletin 30, 33 p.

Sacks, P. E., and Platt, L. B., 1985, Depth and timing of decollement extension, southern Portneuf Range, southeastern Idaho, *in* Kerns, G. J., and Kerns, R. L., Jr., eds., Orogenic patterns and stratigraphy of north-central Utah and southeastern Idaho: Utah Geological Association Publication 14, p. 119–127.

Steely, A. N., Janecke, S. U., Long, S. P., Carney, S. C., Oaks, R. Q., Jr., Langenheim, V. E., and Link, P. K., 2005, Evolution of a Late Cenozoic supradetachment basin above a flat-on-flat detachment with a folded lateral ramp, SE Idaho, *in* Pederson, J., and Dehler, C. M., eds., Interior Western United States: Geological Society of America Field Guide 6, p. 169–198.

Trimble, D. E., 1976, Geology of the Michaud and Pocatello quadrangles, Bannock and Power counties, Idaho: U.S. Geological Survey Bulletin 1400, 88 p., 1 sheet.

Trimble, D. E., and Carr, W. J., 1976, Geology of the Rockland and Arbon quadrangles, Power County, Idaho: U.S. Geological Survey Bulletin 1399, 115 p., 1 sheet.

Veatch, A. C., 1907, Geography and geology of a portion of southwestern Wyoming, with special reference to coal and oil: U.S. Geological Survey Professional Paper 56, 178 p.

Williams, I. S., 1998, U-Th-Pb geochronology by ion microprobe, *in* McKibben, M. A., Shanks, W. C. III, Ridley, W. I., eds., Applications of microanalytical techniques to understanding mineralizing processes: Reviews in Economic Geology, v. 7, p. 1–35.

Williams, I. S., and Claesson, S., 1987, Isotopic evidence for the Precambrian provenance and Caledonian metamorphism of high-grade paragneisses from the Seve Nappes, Scandinavian Caledonides II: Ion microprobe zircon U-Th-Pb: Contributions to Mineralogy and Petrology, v. 97, p. 205–217.

Zoback, M. L., 1983, Structure and Cenozoic tectonism along the Wasatch fault zone, Utah, *in* Miller, D. M., Todd, V. R., and Howard, K. A., eds., Tectonic and stratigraphic studies in the eastern Great Basin: Boulder, Colorado, Geological Society of America Memoir 157, p. 3–27.

Manuscript Submitted July 29, 2005

Revised Manuscript Submitted January 27, 2006

Manuscript Accepted February 26, 2006